Meng-Jiao Wang
Michael Morris

Rubber Reinforcement with Particulate Fillers

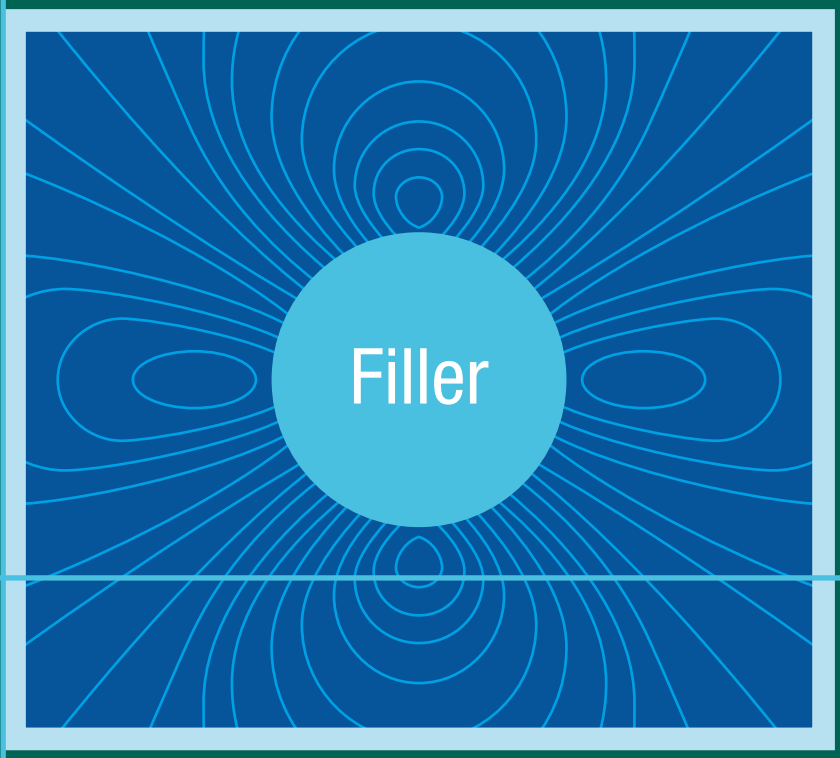

Chemical Industry Press

HANSER

Meng-Jiao Wang
Michael Morris

Rubber Reinforcement with Particulate Fillers


Chemical Industry Press Co., Ltd.

HANSER
Hanser Publications, Cincinnati
Hanser Publishers, Munich

The Authors:

Meng-Jiao Wang, EVE Rubber Institute, Zhengzhou Road, Qingdao, China

Michael Morris, Cabot Corporation, Billerica, MA 01821, USA

Distributed in the Americas by:
Hanser Publications
414 Walnut Street, Cincinnati, OH 45202 USA
Phone: (800) 950-8977
www.hanserpublications.com

Distributed in all other countries by:
Carl Hanser Verlag
Postfach 86 04 20, 81631 Munich, Germany
Fax: +49 (89) 98 48 09
www.hanser-fachbuch.de

Library of Congress Control Number: 2020943840

Editor: Dr. Mark Smith
Coverconcept: Marc Müller-Bremer, www.rebranding.de, Munich
Coverdesign: Max Kostopoulos
Typesetting: Beijing Keyin Company
Printed and bound by Beijing Hucais Culture Communication Co., Ltd
Printed in Beijing, China

ISBN: 978-1-56990-719-1
E-Book ISBN: 978-1-56990-720-7

Preface

Soon after rubber's discovery as a remarkable material in the 18th century, the application of particulate fillers − alongside vulcanization − became the most important factor in the manufacture of rubber products, with the consumption of these particulate fillers second only to rubber itself. Fillers have held this important position not only as a cost savings measure by increasing volume, but more importantly, due to their unique ability to enhance the physical properties of rubber, a well-documented phenomenon termed "reinforcement." In fact, the term filler is misleading because for a large portion of rubber products, tires in particular, the cost of filler per unit volume is even higher than that of the polymer. This is especially true for the reinforcement of elastomers by extremely fine fillers such as carbon black and silica. This subject has been comprehensively reviewed in the monographs "Reinforcement of Elastomers," edited by G. Kraus (1964), "Carbon Black: Physics, Chemistry, and Elastomer Reinforcement," written by J.-B. Donnet and A. Voet (1975), and "Carbon Black: Science and Technology," edited by J.-B. Donnet, R. C. Bansal, and M.-J. Wang (1993). There has since been much progress in the fundamental understanding of rubber reinforcement, the application of conventional fillers, and the development of new products to improve the performance of rubber products.

While all agree that fillers as one of the main components of a filled-rubber composite have the most important bearing on improving the performance of rubber products, many new ideas, theories, practices, phenomena, and observations have been presented about how and especially why they alter the processability of filled compounds and the mechanical properties of filled vulcanizates.

This suggests that the real world of filled rubber is so complex and sophisticated that multiple mechanisms must be involved. It is possible to explain the effect of all fillers on rubber properties ultimately in similar and relatively nonspecific terms, i.e., the phenomena related to all filler parameters should follow general rules or principles. It is the authors' belief that, regarding the impact of filler on all aspects of rubber reinforcement, filler properties, such as microstructure, morphology, and surface characteristics, play a dominant role in determining the properties of filled rubbers, hence the performance of rubber products, via their effects in rubber. These effects, which include hydrodynamic, interfacial, occlusion, and agglomeration of fillers, determine the structure of this book.

The first part of the book is dedicated to the basic properties of fillers and their characterization, followed by a chapter dealing with the effect of fillers in rubber. Based on these two parts, the processing of the filled compounds and the properties of the filled vulcanizates are discussed in detail. The last few chapters cover some special applications of fillers in tires, the new development of filler-related materials for tire applications, and application of fumed silica in silicone rubber. All chapters emphasize an internal logic and consistency, giving a full picture about rubber reinforcement by particulate fillers. As such, this work is intended for those working academically and industrially in the areas of rubber and filler.

We would like to express our heartfelt thanks to Wang's colleagues at the EVE Rubber Institute Mr. Weijie Jia, Mr. Fujin He, Dr. Bin Wang, Dr. Wenrong Zhao, Dr. Hao Zhang, Dr. Mingxiu Xie, Dr. Yudian Song, Dr. Feng Liu, Dr. Liang Zhong, Dr. Bing Yao, Dr. Dan Zhang, Dr. Kai Fu, and Mr. Shuai Lu for their assistance in preparing this book. Special thanks are due to the EVE Rubber Institute, Qingdao, China and Cabot Corporation, USA. Without their firm backing and continuous understanding, this effort could not have been accomplished.

Meng-Jiao Wang, Sc. D., Professor
EVE Rubber Institute, Qingdao, China

Michael Morris, Ph. D., Cabot Corporation
Billerica, Massachusetts USA

About the Authors

Meng-Jiao Wang began his career in rubber research in 1964 after graduating from Shandong University and joining the Beijing Research and Design Institute of the Rubber Industry, China, where his last position was a professor and chief engineer. In 1982, he moved to France to work at the CNRS in Mulhouse as an associate researcher. He was awarded a doctoral degree (Docteur d'Etat es Sciences) in 1984. He then spent a year and half as a visiting scientist working at the University of Akron. From 1988 to 1989 he worked at the German Institute for Rubber Technology (DIK) as a visiting scientist and later he joined Degussa as a Senior Scientist. In 1993, Dr. Wang moved again to the United States to join Cabot, and soon became a scientific fellow of the company. From 2011 onwards, he has been the scientific fellow of National Engineering Research Center for Rubber and Tire and the director of the EVE Rubber Institute, China.

Over his 56-year career in rubber research, Meng-Jiao Wang has published over 140 scientific papers and 10 book chapters, and he has 55 different US and Chinese patents and 24 equivalent international patents to his name. He co-edited the book "Carbon Black: Science and Technology" and co-authored 6 other books. He was previously a member of the Editorial Board of the journal *Rubber Chemistry and Technology* (USA).

Michael Morris is currently a Principal Scientist at Cabot Corporation in Massachusetts, USA. He was awarded a Ph.D. from the University of Southampton, UK, in 1985 and began his career in rubber research at the Malaysian Rubber Producers Research Association (MRPRA; now TARRC) the same year. In 1987, he was seconded to the Rubber Research Institute of Malaysia in Kuala Lumpur to work on various aspects of natural rubber research. After four years, in 1991, he returned to the MRPRA and continued research, mainly on NR latex. In 1996, Dr. Morris moved to the USA to join the R&D organization of Cabot Corporation. His research and applications development were

initially focused on fumed silica, as part of the Cab-O-Sil division. Since 2005, he has been part of the rubber reinforcement group at Cabot, focused on carbon black reinforcement of rubber.

During his career, Michael Morris has published 18 journal papers, 2 book chapters, and 14 conference presentations. In addition, he is an inventor on 12 granted US patents and numerous other international patents.

Contents

1 Manufacture of Fillers

The history of particulate fillers used in rubber is almost as long as that of rubber itself[1–3]. One aspect of filler addition has been improvement of rubber properties. Another aspect was extension of the rubber with less expensive materials. After Hancock developed the earliest device using rollers to crumb natural rubber (NR) in 1820, and the two-roll mill for NR mastication and compounding was patented by Chaffee in 1836 and 1841, incorporation of inert fillers in finely divided particulate form became standard practice. Fillers such as ground limestone, barites, clay, kaolin, etc. were used in order to extend and cheapen the compounds since it was found that in natural rubber, quite a bit of filler could be added without detracting too much from the final vulcanizate properties. Zinc oxide was originally used for its whiteness, and later was found to have some reinforcing effect, becoming known as an "active" filler. Carbon black, which was known as a black pigment, was also found to be able to improve the rubber properties significantly at low concentrations, especially the stiffness. Systematic studies of the effect of fillers had been reported by Heinzerling and Pahl in Germany in 1891. Part of this effect may be due to its activating effect on many vulcanization accelerators for which zinc oxide is still utilized. In 1904, Mote in England, discovered the reinforcing effect of carbon black. He reported that the tensile strength of the filled NR increased drastically, compared with the values obtained with the techniques of that time. Although automobiles had been around and running on rubber tires for more than a decade, the importance of this discovery was recognized and developed when black tires were demonstrated to have better wear resistance than white ones, which contained mainly zinc oxide as a filler. Carbon black is now the most important filler used in rubber. In the last century, the production techniques and designation of types of carbon black have developed rapidly.

In the meantime, non-black fillers have also developed. Among these non-black ones, the first reinforcing filler, calcium silicate, was introduced in 1939. It was prepared by wet precipitation from sodium silicate solution with calcium chloride. In further development of the process, the calcium was leached out by hydrochloric acid to yield a reinforcing silica pigment of comparable particle size. About 10 years later, direct precipitation of silica from sodium silicate solution had developed to a commercial process and this is still a major process today. In 1950, a different type of anhydrous silica appeared, which was made by reacting silicon tetrachloride or silica chloroform

(trichlorosilane) with water vapor in a hydrogen-oxygen flame. Because of the high temperature at the formation (about 1400°C), this pyrogenic silica has a lower concentration of silanol groups on the surface than the precipitated silicas. The latter contain about 88%−92% SiO_2 and have ignition losses of 10%−14%, whereas pyrogenic silica contains 99.8% silica. Because of its lower surface concentration of silanols, ultra-high purity with total impurities in many cases below 100 ppm (parts per million), and much higher price, pyrogenic silica is mainly used as a filler for high cost compounds such as silicone rubber.

In contrast, since the beginning of the industrial-scale production of fine-particle silicas and silicates in 1948, precipitated silica manufacturers have always desired to find their products used in tires as well. Whereas silicas were rapidly able to replace up to 100 percent of carbon black in shoe sole materials and also made their way into the mechanical goods sector, mostly as blends with carbon blacks, their use in tires in any quantities worth mentioning has long been limited to two types of compounds: off-the-road tread compounds containing 10 phr to 15 phr of silica blended with carbon black in order to improve tear properties, and textile and steel cord bonding compounds containing 15 phr of silica, again blended with carbon black, in combination with resorcinol/formaldehyde systems[4].

During the two oil crises in the 1970s, which had led to a steep rise in the price of carbon black, the question arose whether silica in tires could be an alternative to carbon black. When the price of oil fell and the fear of a lack of availability of carbon blacks subsided, this question was soon forgotten, especially since the price of silica was always higher than that of carbon black, at least in Japan and the USA. Experience has shown that silicas only have a chance to be used in tires if they offer technological advantages which are superior to those of carbon blacks.

Two developments have created a new opportunity for silicas to be used in tires: the increased awareness of the pollution from industry and the necessity of protecting the environment have given rise to a call for tires combining a long service life with driving safety and low fuel consumption. The introduction of bifunctional organosilanes as coupling agents now permits the reinforcing mechanism of silicas to be controlled by chemical means[4,5]. Based on systematic studies of surface characteristics, polymer-filler interactions, and better understanding of compounding and processing, silica was successfully used to replace carbon black as the principal filler in the tread compound of the “green tire” patented in 1992[6]. Since then, the application of precipitated silica in tire has been continuously growing, not only in tread compounds, but also in other parts of tires.

In the last two decades, research on rubber reinforcement with particulate fillers and the development of new fillers have been very hot. Since the main fillers used in the rubber industry are still carbon blacks and silicas, the topics of this book will focus on these two materials and their derivatives.

1.1 Manufacture of Carbon Black

The history of carbon black manufacture is very long, such as in China, about 3000 B.C., carbon black for pigment use was made by burning vegetable oils in small lamps and collecting the carbon on a ceramic lid; in Egypt, carbon black was used as a pigment for paints and lacquers. Starting in 1870, natural gas began to be used as the feedstock for carbon black manufacture. Over a couple of decades, the channel process was developed in which small gas flames burning in restricted air supply impinged on iron channels. In 1976, the last channel black plant was closed in the USA, due to the pollution of smoke plumes.

A critical event in the development of the carbon black industry was the discovery of the benefits of carbon black as a reinforcing agent for rubber in 1904[1]. As the automobile became ubiquitous during the 1920s, the application of pneumatic tires grew rapidly and soon by-passed other applications, causing rapid growth in consumption of carbon black. Also in the 1920s, two other processes concerning carbon black production were introduced, both using natural gas as feedstock, but having better yields and lower emissions than the channel process. One was the thermal black process, in which a brick checker is employed and works alternately by absorbing heat from a natural gas air flame, and then giving up heat to crack natural gas to carbon and hydrogen. The other process was the gas furnace process, which is no longer practiced.

The oil furnace process was first introduced by Phillips Petroleum at its plant in Borger, Texas, in 1943. This process rapidly replaced all others for the production of carbon black for use in rubber. In a modern version of the oil furnace process, carbon black yields range from 65% downward depending on the surface area of the product. Product recovery is essentially 100% as a result of high efficiency bag filters. The overwhelming majority of carbon black reactors today are based on the oil furnace process.

1.1.1 Mechanisms of Carbon Black Formation

The formation of particulate carbon involves either pyrolysis or incomplete combustion of hydrocarbon materials. Enormous literature has been published to describe the mechanism of carbon black formation, from a series of lectures by Michael Faraday at the Royal Institution in London in the 1840s[2], to a more recent intensive review[7]. Since Faraday's time, many theories have been proposed to account for carbon formation, but controversy still exists regarding the mechanism.

Mechanisms of carbon black formation must account for the experimental observations of the unique morphology and microstructure of carbon black. These include the presence of nodules, or particles, multiple growth centers within some nodules, the fusion of nodules into large aggregates, and the paracrystalline or concentric layer

plane structure of the aggregates. It is generally accepted that the mechanism of formation involves a series of stages as follows:

Formation of gaseous carbon black precursors at high temperature – This involves dehydrogenation of primary hydrocarbon molecular species to atomic carbon or primary free radical and ions which condense to semi-solid carbon precursors (or poly-nuclear-aromatic sheet) and/or formation of large hydrocarbon molecules by polymerization which then is dehydrogenated to particle precursors[3]. Taking production of furnace black with high aromatic feedstock as an example, Figure 1.1 represents several of the possible paths that feedstock can take as it is mixed with the primary fire in the reactor at the early stage. The primary fire has excess oxygen, carbon dioxide, and water, all of which act as combustion (or oxidation) reactants to the feedstock molecules. These molecules can react with and break up any feedstock molecules into small combustion species; any feedstock that goes this route is lost for carbon black production. As there is a limit to oxidative species, the remaining feedstock can either be broken down by pyrolysis or survive and become directly involved in carbon black formation reactions. Typical pyrolysis species are hydrogen, acetylene, and polyynes, which are essentially chained acetylenes. At least two formation paths are thought to occur. The first one is ring growth from acetylene, polyyne,or polycyclic aromatic hydrocarbon (PAH) collision with PAH molecules. When the number of rings reaches five or six, the molecules become thermally stable and will only be attacked by remaining oxidant molecules. These PAH molecules will

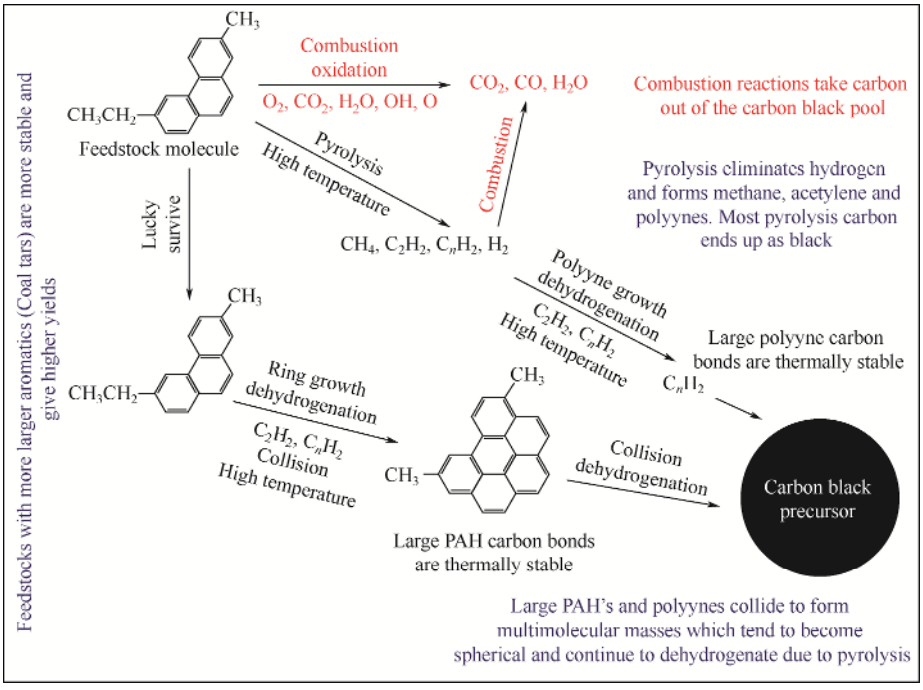

Figure 1.1 Formation of gaseous carbon black precursors

eventually stack up after collisions and then begin to form the crystallites which are found in the finished primary particles. The other route to carbon black occurs as the acetylene polymerizes (polyacetylene) to form long chain polyynes which also reach a thermally stable size and begin to collide with the large PAH molecules. These polyynes can then restructure themselves to increase the crystallite size or provide the amorphous portion of the carbon black particles. Once these particles grow to about one to two nanometers they tend to become spherical and are referred to as carbon black precursors.

Nucleation – Because of increasing mass of the carbon particle precursors through collision, the larger fragments are no longer stable and condense out of the vapor phase to form nuclei or growth centers.

Particle growth and aggregation – In this period, three processes go on simultaneously as shown in Figure 1.2: condensation of more carbon precursors on the existing nuclei, coalescence of small particles into larger ones, and formation of new nuclei. Coalescence and growth seem to predominate. The products of this stage are "proto-nodules".

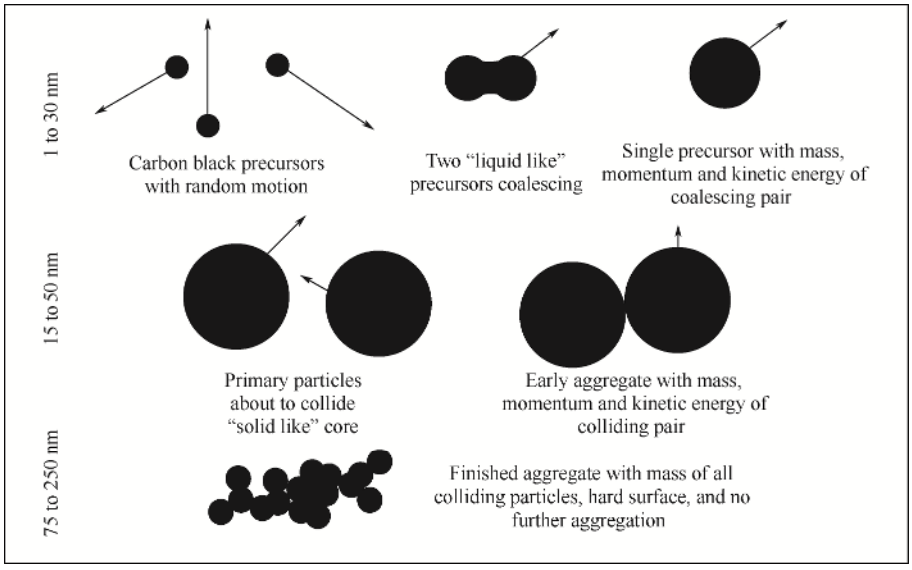

Figure 1.2 Particle growth and aggregation

Surface growth – Surface growth includes the processes in which the small species attach to or deposit on the surfaces of existing particles or aggregates, forming the nodules and aggregates with their characteristic onion micro-structure (note: aggregates are permanent structures cemented by carbon). The surface growth represents about 90% of total carbon yield. It is responsible for the stability of the aggregates because of the continuous carbon network formation. Aggregates are formed and cemented in this stage.

Agglomeration – Once no more carbon is forming and aggregation ceases, aggregates collide and adhere by van der Waals forces but there is no material to cement them together, hence they form temporary structures (agglomerates).

Aggregate gasification – After its formation and growth, the carbon black surface undergoes reaction with the gas phase, resulting in an etched surface. Species such as CO_2, H_2O, and of course any residual oxygen attack the carbon surface. The oxidation is determined by gas phase conditions, such as temperature, oxidant concentration, and flow rates.

Practically, the carbon black morphology and surface chemistry can be well-controlled by changing the reaction parameters. For furnace carbon blacks, the reaction temperature is the key variable that governs the surface area. The higher the temperature, the higher is the pyrolysis rate and the more nuclei are formed, resulting in an earlier stop of the growth of the particles and aggregates due to the limitation of starting materials. Therefore, with higher reaction temperature, achieved by adjusting air rate, fuel rate, and feedstock rate, the surface area of carbon black can be increased. Addition of alkali metal salts into the reactor can modify the aggregation process, influencing carbon black structure. At the reactor temperature, the salts of alkali metals, such as potassium, are ionized. The positive ions adsorb on the forming carbon black nodules and provide some electrostatic barrier to internodule collisions, resulting in lower structure[8].

The time scale of carbon black formation varies substantially across the range of particle sizes found in commercial furnace blacks. For blacks with surface areas around 120 m^2/g, the carbon black formation process from oil atomization to quench takes less than 10 milliseconds. For blacks with surface areas around 30 m^2/g, formation times are a few tenths of a second.

1.1.2 Manufacturing Process of Carbon Black

1.1.2.1 Oil-Furnace Process

The oil-furnace process accounts for over 95 percent of all carbon black produced in the world. It was developed in 1943 and rapidly displaced previous gas-based technologies because of its higher yields and the broader range of blacks that could be produced. It also provides highly effective capture of particulates and has greatly improved the environment around carbon black plants. As indicated in the mechanism discussion, it is based on the partial combustion of residual aromatic oils. Because residual oils are ubiquitous and are easily transported, the process can be practiced with little geographic limitation. This has allowed construction of carbon black plants all over the world. Plants are typically located in areas of tire and rubber goods manufacture. Because carbon black is of relatively low density, it is far less expensive to transport feedstock oil than to transport the black.

For nearly 80 years since its invention, the oil-furnace process has undergone several cycles of improvement. These improvements have resulted in increased yields, larger

process trains, better energy economy, and enhanced product performance. A simplified flow diagram of a modern furnace black production line is shown in Figure 1.3[9]. This is intended to be a generic diagram and contains elements from several operators' processes. The principal pieces of equipment are the air blower, process air and oil preheaters, reactors, quench tower, bag filter, pelletizer, and rotary dryer. The basic process consists of atomizing the preheated oil in a combustion gas stream formed by burning fuel in preheated air. The atomization is carried out in a region of intense turbulent mixing. Some of the atomized feedstock is combusted with excess oxidant in the combustion gas. Temperatures in the region of carbon black formation range from 1400°C to over 1800°C. The details of reactor construction vary from manufacturer to manufacturer and are confidential to each manufacturer. Leaving the formation zone, the carbon black containing gases are quenched by spraying water into the stream. The partially cooled smoke is then passed through a heat exchanger where incoming air is preheated. Additional quench water is used to cool the smoke to a temperature consistent with the life of the bag material used in the bag filter. The bag filter separates the unagglomerated carbon black from the by-product tail gas which contains nitrogen, hydrogen, carbon monoxide, carbon dioxide, and water vapor. It is mainly nitrogen and water vapor. The tail gas is frequently used to fuel the dryers in the plant, to provide other process heat, or sometimes is burned to manufacture steam and electric power either for internal plant use or for sale.

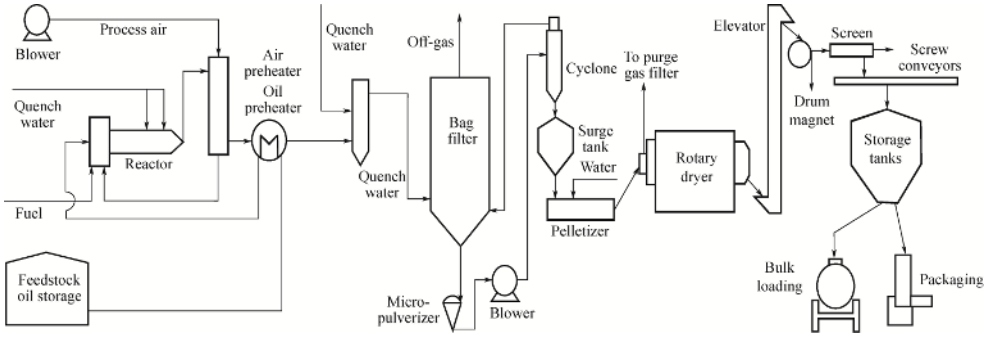

Figure 1.3 Flow diagram of a modern furnace black process

The fluffy black from the bag filter is mixed with water, typically in a pin mixer, to form wet granules. These are dried in a rotary dryer, and the dried product is conveyed to bulk storage tanks. For special purposes, dry pelletization in rotary drums is also practiced. Most carbon black is shipped by rail or in bulk trucks. Various semi-bulk containers are also used including IBC's and large semi-bulk bags. Some special purpose blacks are packed in paper or plastic bags.

While the reactor and its associated air-moving and heat-exchange equipment are where the properties of the black are determined, they tend to be dwarfed by the bag collectors, the dryers, and particularly the storage tanks.

Feedstocks

Feedstocks for the oil-furnace process are heavy fuel oils. Preferred oils have high aromaticity, are free of suspended solids, and have a minimum of asphaltenes. Suitable oils are catalytic cracker residue (once residual catalyst has been removed), ethylene cracker residues, and distilled heavy coal tar fractions. Other specifications of importance are freedom from solid materials, moderate to low sulfur, and low alkali metals. The ability to handle such oils in tanks, pumps, transfer lines, and spray nozzles is also a primary requirement.

Reactor

The heart of a furnace black plant is the furnace or reactor where carbon black formation takes place under high temperature, partial combustion conditions. The reactors are designed and constructed to be as trouble-free as possible over long periods of operation under extremely aggressive conditions. They are monitored constantly for signs of deterioration in order to ensure constant product quality. The wide variety of furnace black grades for rubber and pigment applications requires different reactor designs and sizes to cover the complete range, though closely related grades can be made in the same reactor by adjusting input variables. Reactors for higher surface area and reinforcing grades operate under high gas velocities, temperatures, and turbulence to ensure rapid mixing of reactant gases and feedstock. Lower surface area and less reinforcing grades are produced in larger reactors at lower temperatures, lower velocities, and longer residence time. Table 1.1 lists carbon formation temperatures, and residence times for the various grades of rubber blacks.

Table 1.1 Reactor conditions for various grades of carbon blacks

Black	Surface area/(m^2/g)	Temperature/°C	Residence time/s	Maximum velocity/(m/s)
N100 series	145	1800	0.008	
N200 series	120		0.010	180–400
N300 series	80	1550	0.031	
N500 series	42		1	30–80
N700 series	25	1400	1.5	0.5–1.5
N990 thermal	8	1200–1350	10	10

A key development in the carbon black reactor technology was the development of the zoned axial flow reactor for reinforcing blacks in the early 1960s[8]. The reactor consists of three zones. The first zone is a combustion zone in which fuel and air are completely burned to produce combustion gases with excess oxygen. This gas flow is accelerated to high velocity in a throat zone with intense turbulent mixing. The feedstock is injected either into this throat zone or just ahead; therefore, the reacting gases issue from the throat into a second cylindrical zone as a turbulent diffusion jet.

Depending on the desired black, the jet may be allowed to expand freely, or may be confined by bricking. Downstream of the reaction zone is a water quench zone. The throughput of a single reactor train varies from manufacturer to manufacturer and with grade of black. The largest reactors in operation have capacities of over 30,000 metric tons per year. Many producers operate smaller reactors in parallel. Reactors are typically designed to make a series of related blacks. Air and gas may be introduced to the primary combustion zone either axially, tangentially, or radially. The feedstock can be introduced into the primary fire either axially or radially in the high velocity section of the mixing zone. The high velocity section may be Venturi-shaped or consist of a narrow diameter choke. Plants may have from one to several operating trains.

Carbon black reactors are made of carbon steel shells lined with several courses of refractory. The most severe services are in the combustor and in the throat zone. Different manufacturers take different approaches to these elements, some using exotic materials or selected water cooled metal surfaces, others using conventional materials and limiting temperatures to what their materials can stand. Most manufacturers achieve refractory life of one to several years. For the rubber grade carbon blacks, at least three different reactor designs must be used to make this range of furnace blacks. Figure 1.4 and Figure 1.5 show the designs of commercial reactors found in patents.

The quality and yield of carbon black depend on the quality and carbon content of the feedstock, the reactor design, and the input variables. Surface area in particular is controlled by adjusting the temperature in the reaction zone. Structure is adjusted by introducing potassium into the combustion gas. This may be done in any of a variety of ways.

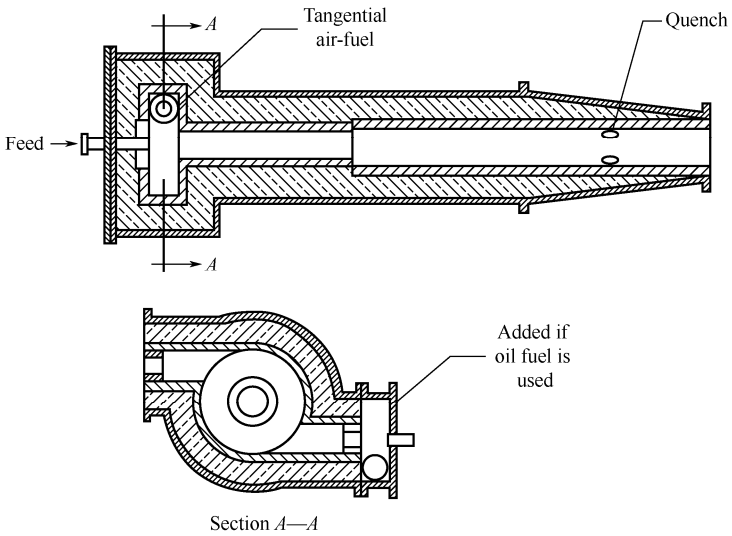

Figure 1.4 Reactor for N300–N200 carbon blacks[10]

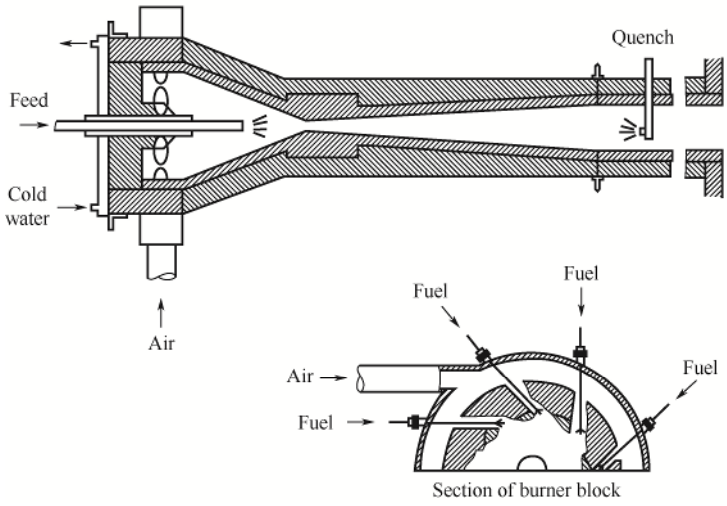

Figure 1.5 Reactor for tread blacks[11]

The energy utilization in the production of one kilogram of oil-furnace carbon black is in the range of $(9-16)\times10^7$ J, and the yields are 300−660 kg/m^3 depending on the grade. The energy inputs to the reactor are the heat of combustion of the preheated feedstock, heat of combustion of natural gas, and the thermal energy of the preheated air. The energy output consists of the heat of combustion of the carbon black product, the heat of combustion and the sensible heat of the tail gas, the heat loss from the water quench, the heat loss by radiation to atmosphere, and the heat transferred to preheat the primary combustion air.

1.1.2.2 The Thermal Black Process

Thermal black is a large particle size and low structure carbon black made by the thermal decomposition of natural gas, coke oven gas, or liquid hydrocarbons in the absence of air or flames. Its economic production requires inexpensive natural gas. Today it is among the most expensive of the blacks regularly used in rubber goods. It is used in rubber and plastics applications for its unique properties of low hardness, high extensibility, low compression set, low hysteresis, and excellent processability. Its main uses are in O-rings and seals, hose, tire inner liners, V-belts, other mechanical goods, and in cross-linked polyethylene for electrical cables.

The thermal black process dates from 1922. The process is cyclic using two refractory-lined cylindrical furnaces or generators about 4 m in diameter and 10 m high. During operation, one generator is being heated with a near stoichiometric ratio of air and off-gas from the making generator whereas the other generator, heated to an average temperature of 1300°C, is fed with natural gas. The cycle between black production and heating is five minutes alternating between generators, resulting in a reasonably continuous flow of product and off-gases to downstream equipment. The effluent gas from the make cycle, which is about 90% hydrogen, carries the black to a quench

tower where water sprays lower the temperature before entering the bag filter. The effluent gas is cooled and dehumidified in a water scrubber for use as fuel in the heating cycle. The collected black from the filters is conveyed to a magnetic separator, screened, and hammer-milled. It is then bagged or pelletized. The pelletized form is bagged or sent to bulk loading facilities.

1.1.2.3 Acetylene Black Process

The high carbon content of acetylene (92%) and its property of decomposing exothermically to carbon and hydrogen make it an attractive raw material for conversion to carbon black. Acetylene black is made by a continuous decomposition process at atmospheric pressure and temperatures of 800−1000°C in water-cooled metal retorts lined with refractory. The process consists of feeding acetylene into the hot reactors. The exothermic reaction is self-sustaining and requires water cooling to maintain a constant reaction temperature. The carbon black-laden hydrogen stream is then cooled, followed by separation of the carbon from the hydrogen tail gas. The tail gas is either flared or used as fuel. After separation from the gas stream, acetylene black is very fluffy with a bulk density of only 19 kg/m^3. It is difficult to compact and resists pelletization. Commercial grades are compressed to various bulk densities up to 200 kg/m^3.

Acetylene black is very pure with a carbon content of 99.7%. It has a surface area of about 65 m^2/g, an average particle diameter of 40 nm, and a very high but rather weak structure with a DBP number of 250 mL/100 g. It is the most crystalline or graphitic of the commercial blacks. These unique features result in high electrical and thermal conductivity, low moisture adsorption, and high liquid absorption.

A significant use of acetylene black is in dry cell batteries where it contributes low electrical resistance and high capacity. In rubber it gives electrically conductive properties to heater pads, tapes, antistatic belt drives, conveyor belts, and shoe soles. It is also useful in electrically conductive plastics such as electrical magnetic interference (EMI) shielding enclosures. Its contribution to thermal conductivity has been useful in rubber curing bags for tire manufacture.

1.1.2.4 Lampblack Process

The lampblack process has the distinction of being the oldest and most primitive carbon black process still being practiced. The ancient Egyptians and Chinese employed techniques similar to modern methods collecting the lampblack by deposition on cool surfaces. Basically, the process consists of burning various liquid or molten raw materials in large, open, shallow pans 0.5−2 m in diameter and 16 cm deep under brick-lined flue enclosures with a restricted air supply. The smoke from the burning pans passes through low velocity settling chambers from which the carbon black is cleared by motor-driven ploughs. In more modern installations, the black is separated by cyclones and filters. By varying the size of the burner pans and the amount of combustion air, the particle size and surface area can be controlled within narrow limits. Lampblacks have similar properties to the low surface area oil-furnace

blacks. A typical lampblack has an average particle diameter of 65 nm, a surface area of 22 m^2/g, and a DBP number of 130 mL/100 g. Its main use is in paints, as a tinting pigment where blue tone is desired. In the rubber industry lampblack finds some special applications.

1.1.2.5 Impingement (Channel, Roller) Black Process

From World War I to World War II the channel black process made most of the carbon black used worldwide for rubber and pigment applications. The last channel black plant in the United States was closed in 1976. The demise of channel black was caused by environmental problems, cost, smoke pollution, and the rapid development of oil-furnace process grades that were equal or superior to channel black products particularly for use in synthetic rubber tires.

The name channel black came from the steel channel irons used to collect carbon black deposited by small natural gas flames impinging on their surface iron channels. Today tar fractions are used as raw material in addition to natural gas. In modern installations channels have been replaced by water cooled rollers. The black is scraped off the rollers, and the off-gases from the steel box enclosed rollers are passed through bag filters where additional black is collected. The purified exhaust gases are vented to the atmosphere. The oils used in this process must be vaporized and conveyed to the large number of small burners by means of a combustible carrier gas. Yield of rubber-grade black is 60%, and 10%−30% for high quality color grades.

The characteristics of roller process impingement blacks are basically similar to those of channel blacks. They have an acidic pH, a volatile content of about 5%, surface area of about 100 m^2/g, and an average particle diameter of 10−30 nm. The smaller particle size grades are used as color (pigment) blacks, and the 30 nm grade is used in rubber.

1.1.2.6 Recycle Blacks

The pyrolysis of carbon black-containing rubber goods has been promoted as a solution to the accumulation of waste tires. In the processes in question, tires are pyrolyzed in the absence of oxygen, usually in indirect fired rotary kiln type units. The rubber and extender oils are cracked to hydrocarbons which are collected and sold as fuels or petrochemical feedstocks. The gaseous pyrolysis products are burned as fuel for the process. Steel tire cord is removed magnetically and the remainder of the residue is milled into a “pyrolysis black”. This contains the carbon black, silica, and other metal oxides from the rubber and some newly created char. Typically these materials have 8% to 10% ash, and contain a lot of coarse residue. Most are difficult to pelletize. They have, on average, the reinforcing properties of a N300 black. But because they are a mixture of N600 and N700 blacks with N100 and N200 blacks, they are not particularly suitable for either reinforcing or semi-reinforcing applications. To-date they find application in relatively non-demanding uses such as playground and floor mats.

1.1.2.7 Surface Modification of Carbon Blacks

For the most of its long history, the carbon black industry had concentrated on morphology as the key factor controlling product performance and grade differentiation. Scientists have only recently recognized the importance of interface composition between the carbon blacks and the medium in the composite where the carbon black is used.

The early stages of surface modification can be traced back to the 1940s and 1950s. The approaches include physical adsorption of some chemicals on the carbon black surface, heat treatment, and frequently oxidation. During the 1980s and 1990s, some work on plasma treatment was reported. For chemical and polymer grafting modifications, a great deal of academic work was done in the 1950s and 1960s in France, US, and Japan, using surface oxygen groups as functional groups. However, because of rapid development of applications of carbon black in different areas and the challenge from other reinforcing particles in its traditional applications, surface modification technologies for carbon black have been developing very rapidly over the last decades. These include surfactant treated surfaces, chemically modified surfaces, and deposition of other phases during or after black formation. Today there is active commercial development and new product introduction in all areas.

1.1.2.7.1 Attachments of the Aromatic Ring Nucleus to Carbon Black

Two approaches characterize this area. A number of patents have been issued to Cabot Corporation[12,13], which describe that the decomposition of a diazonium compound derived from a substituted aromatic or aliphatic amine results in the attachment of a substituted aromatic ring or chain onto the surface of the carbon black. This results in a stable attachment which is not sensitive to moisture. Examples show attachment of amines, anionic and cationic moieties, polysulfide moieties that can be attached into an elastomer network, and alkyl, polyethoxyl, and vinyl groups. Practically, the surface chemistry and physical chemistry can be tailored according to the applications of carbon blacks. Some applications are claimed in aqueous media for dispersion[14], in oil based coatings and inks for dispersion[15], and in rubbers for reduction of hysteresis and wear resistance improvement[16]. The initially attached groups can also function as sites for further chemical substitution. Another approach has been developed by Xerox Corporation in which oligomers of polymer are prepared using stable free radical polymerization and these are attached to the carbon black surface by reaction of the stable radical[17].

1.1.2.7.2 Attachments to the Aromatic Ring Structure through Oxidized Groups

The acidic surface groups that result from surface oxidation of carbon black are natural synthons for the attachment of functionality. Generally, chemistry is done through either phenolic or carboxylic acid groups on the surface. Some of these groups are present in most blacks, but their density can be increased by treating with various oxidants such as ozone, nitric acid, or hypochlorite[18–20]. Compared to the previous class, these C−O attachments are somewhat more labile, being particularly susceptible

to hydrolysis. The concept of using phenolic groups as points of attachment for conventional silane treating agents has been described in several patents with the particular aim of attaching polysulfide moieties that can be vulcanized into elastomer networks for hysteresis reduction[21]. Some patents have been issued on using the acidic sites on carbon black surfaces as points of reaction of amines. In the particular case in point, the attachment was used to improve compound stability and dispersion in conductive plastics applications[22].

1.1.2.7.3 Metal Oxide Treatment

The carbon black industry has worked on ways to respond to the challenge of silica in tire treads for low rolling resistance (replacing all or some of the carbon black). Cabot has filed on, and widely published, a class of dual phase fillers in which silica or other metal oxides and carbon are co-formed in a carbon black like reactor[23–26]. In the particular product they describe, the carbon black and silica are intimately intermixed on a scale that is about the same size as the carbon black crystallite. In more recent variants, materials where the silica location is more on the exterior of the particle are described[27]. In these materials, the silica is the minor constituent. The main characteristics of these carbon blacks are their lower filler-filler interactions. Filler-polymer interactions are also increased, but by incorporating coupling agents these interactions can be adjusted as required. These materials are used as fillers for low rolling resistance, higher wet skid resistance, and improved wear resistance in tire treads when used with conventional sulfide-silane coupling agents[28,29], or as fillers for silicone rubber when used with alkyl silane and vinyl silane agents[30]. The patent literature suggests that other applications have been considered as well[31]. Patents have also been issued on coated carbon black made by depositing silica on the black surface in an aqueous solution of sodium silicate by adjusting pH with acid[32–34].

■ 1.2 Manufacture of Silica

There are two families of silicas: natural and synthetic. The former are generally crystallized, such as quartz or diatoms. They have contorted and large particles, even after milling, and do not find their application in rubber industry. By synthesis, it is possible to obtain better-defined particles in shape and especially of submicron size. There are two synthetic processes: pyrohydrolysis and precipitation. Both processes produce amorphous products. The first is performed in a high temperature vapor phase from silicon compounds, principally silicon tetrachloride, air, and hydrogen. The products are called “anhydrous” or fumed silica. They have less than 1.5% each of bound water and adsorbed water, which is defined as volatiles removed at, respectively, 105°C and in vacuum. With the precipitation process, the silicas, prepared by precipitation from water-soluble silicates, have approximately 5% each of bound and adsorbed water.

1.2.1 Mechanisms of Precipitated Silica Formation

The formation of precipitated silica is governed by a complex process in which the soluble silicic species which are present in the solution polymerize and form nuclei which grow to form spherical particles of various sizes, depending on the precipitation conditions, mainly temperature and concentration (Figure 1.6).

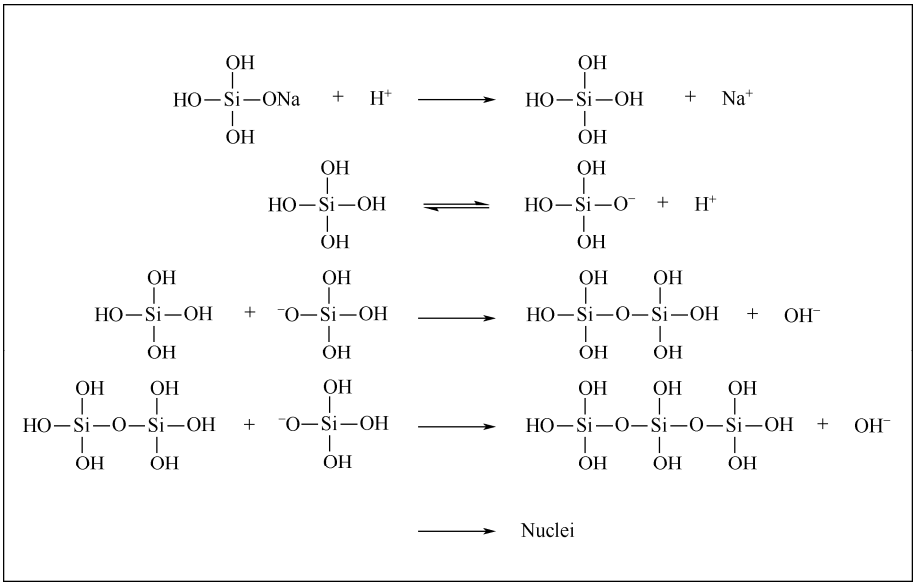

Figure 1.6 Polymerization of silicate

The polymerization, which leads to the formation and the coagulation of colloids, produces silica aggregates. Depending on the reaction conditions, the particles collide with each other forming a gel or aggregates which are then consolidated by further deposition of SiO_2 on their surface as shown in Figure 1.7[35]. Under basic pH conditions, the colloidal particles are negatively charged. They repel each other in an electrostatic way. The electrostatic repulsions are suppressed under the action of an electrolyte such as sodium cation, resulting in the coagulation of the colloidal species. The floc formed is a relatively fragile structure. An addition of water regenerates the colloids. The floc can be made rigid by polymerization of soluble silica on its surface. This is how the silica aggregates are obtained. The morphological characteristics of silica, namely its primary particle size and surface area, determine the shape and size of its aggregates and their distribution. The most important parameters governing the silica morphologies include the proportion of SiO_2 in the alkaline silicate solution, the concentration of the soluble alkali metal salt (such as sodium chloride) in the silicate solution, the reaction temperature, the speed of addition of the acid to the solution, and the other components found in the acid used[36].

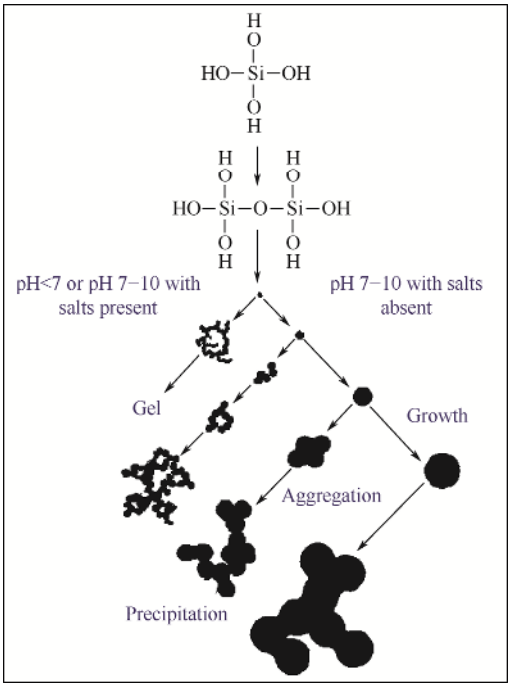

Figure 1.7 Silica formation, growing, and aggregation during precipitation

1.2.2 Manufacturing Process of Precipitated Silica

Fine particle silicas for rubber reinforcement are precipitated by the controlled neutralization of sodium silicate solution by either sulfuric or carbonic acids[36,37]. Their production process is schematically shown in Figure 1.8. The basic raw materials are those required for sodium silicate: quartz sand, sodium carbonate, and water. Sodium silicate (water glass) can be produced in furnace or digester operations, but in either case the ratio of SiO_2 to Na_2O is generally within a range of 2.5−3.5. Practically, the precipitation reaction is carried out in agitated reactors in which the silicate is dissolved, forming a diluted solution. Between pH 3 and 6−7, a silica gel is formed, but the dried silica gel is very difficult to disperse in elastomer systems. The usual pH range for commercial precipitated silica used for elastomer applications is 7.5−9.5 with the optimum being around 8.0−8.5. Above pH 9 there is a high proportion of soluble silica (as silicate) and the remaining precipitate is also extremely fine, which makes filtration extremely difficult. In this case, the filtrate has to be washed to remove the soluble silicate, which is returned as feedstock for subsequent precipitations.

Precipitation produces a low solids-content slurry of silica and sodium sulfate or sodium carbonate from which the salts are removed by washing, either in a counter-current decantation system or during a filter press concentration step. Washing generally reduces the salt content to 1% to 2%. Further concentration in rotary or plate and frame filters produces a solid filtration cake which still contains only 15% to 25%

silica. Because of this high water content the drying step is a large consumer of energy, whether the process involves rotary, tray, belt, flash dryers or spray dryers.

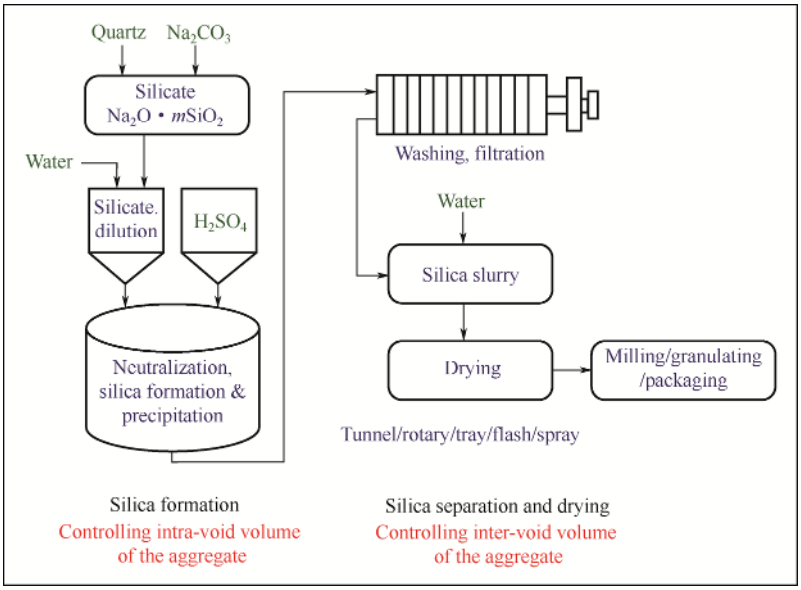

Figure 1.8 Process of precipitated silica production

Generally, the last two dryers are commonly used for rubber silica. With the conventional dryers, the drying is a very slow process at lower temperature. In this case, the aggregates form very tight agglomerates that are very difficult to be dispersed in rubbers.

In the flash drying process, the temperature is usually much higher but the residence time of silica in the dryer is much shorter. During the filtration and drying processes, the silica aggregates bind to each other to form agglomerates. The main distinction between aggregates and agglomerates is related to the nature of the forces between the entities: in aggregates, the particles interact through chemicals bonds whereas in agglomerates, the interactions between aggregates are physical in nature. As will be discussed later, spray drying is the important process for highly dispersible silica.

The process involves producing small hydrated particles which partially explode during the rapid vaporization of water stage. These weakly associated particles are easier to disperse via attrition and infiltration of the dispersing medium. It is essential that during the spray drying process the silica (dry material) is not allowed to reach 180°C, at this temperature condensation of surface silanols starts to occur (moderate rate) which will cause particle-particle fusion and reduced dispersion. The optimum exposure temperature of the dry silica particles is 140−150°C. The air temperature is significantly above this temperature; however, residence time inhibits absorption of heat by the dry particles.

Dry silica is frequently milled and compacted or granulated to attain an optimum balance between dispersibility and dusting.

1.2.3 Mechanisms of Fumed Silica Formation

Fumed silica is generally produced by the vapor phase hydrolysis of chlorosilanes, such as silicon tetrachloride, in a hydrogen-oxygen flame. Such processes are generally referred to as pyrogenic processes. For silicon tetrachloride, the overall reaction is:

$$SiCl_4 + 2H_2 + O_2 \longrightarrow SiO_2 + 4HCl$$

Organosilanes also have been used in pyrogenic processes for the production of fumed silica. In the vapor phase hydrolysis of organosilanes, the carbon-bearing fragments undergo oxidation to form carbon dioxide as a byproduct along with hydrochloric acid.

Ulrich[38] gave a description of the flame process based on the immediate formation of protoparticles directly related to the chemical reaction − rather than surface deposition. At high flame temperatures collision and coalescence of protoparticles lead to the formation of primary particles. The rate of coalescence depends on the viscosity of the molten oxide, which is exceedingly high for silicon dioxide at a flame temperature of about 1500 K. Then the fumed silica primary particles collide and fuse to form three-dimensional, branched, chain-like aggregates. The properties of the silica formed are strongly related to the flame temperature. At lower temperature, collision and sticking of primary particles only results in partial fusion and stable particle aggregates are formed. The silica aggregates leave the flame and cool, but they still collide. As their surfaces are now solid, agglomerates of aggregates are formed that are held together by physico-chemical surface interactions (Figure 1.9).

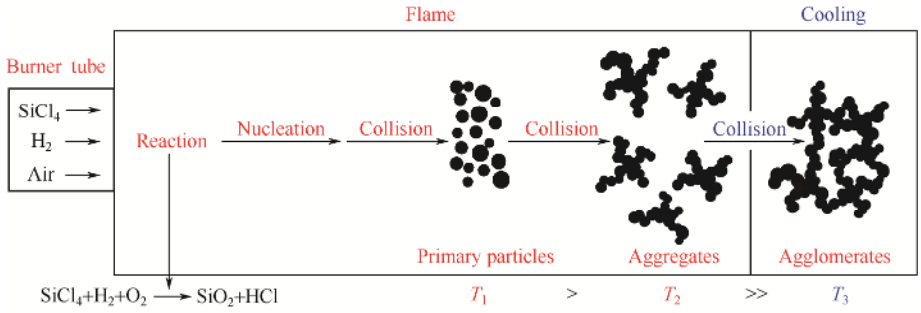

Figure 1.9 Fumed silica formation, growing, and aggregation during production process[39]

1.2.4 Manufacture Process of Fumed Silica

Numerous methods have been developed to produce fumed silica via pyrogenic processes[39–41]. Figure 1.10 describes a process for the pyrogenic production of fumed silica. In accordance with this process, a gaseous feedstock consists of a fuel, such as hydrogen or methane, oxygen, or air, and a volatile silicon compound, such as silicon tetrachloride, wherein the oxygen is present in a stoichiometric or hyper-stoichiometric

proportion. The feedstock is fed to a flame supported by a burner at various flow rates to produce fumed silica. The volume ratios of the individual gas components are reported not to be of critical importance. The molar ratio of the organosilane to the water-forming gases generally is said to be in the range from 1:0 to 1:12, preferably from 1:3 to 1:4.5. Water formed by the combustion of the fuel in oxygen reacts with the silicon tetrachloride to produce silicon dioxide particles, which coalesce and aggregate to form fumed silica. The effluent from the burner is cooled, and the fumed silica is then collected.

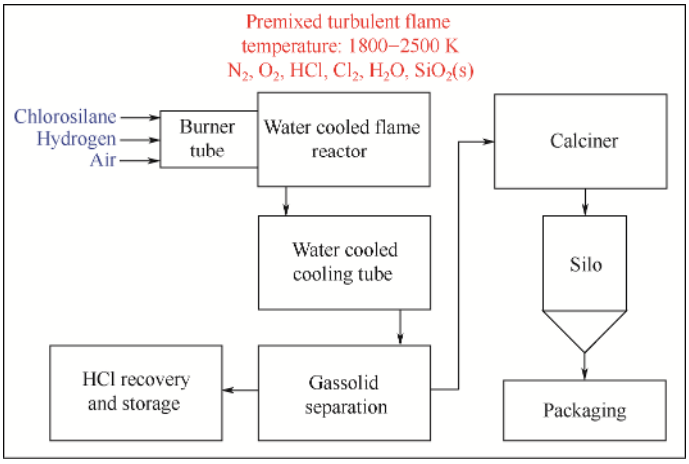

Figure 1.10 Production process of fumed silica

References

[1] Dannenberg E M. The Carbon Black Industry: Over a Century of Progress, Rubber World Mag. Spec. Pub.-Rubber Div. 75th Anniv. (1907-1984).

[2] Faraday M. The Chemical History of a Candle. New York: Viking Press, 1960.

[3] Wang M-J, Gray C A, Reznek S A, et al."Carbon Black" Encyclopedia of Chemical Technology, vol. 4, p. 761, 2004.

[4] Wolff S, Görl U, Wang M-J, et al. Silica-based Tread Compounds: Background and Performance. Paper presented at *TyreTech'93 Conference*, Basel, Switzerland, October 28-29, 1993.

[5] Wolff S, Görl U, Wang M-J, et al. Silane modified silicas. European Rubber Journal, 1994, 16.

[6] Roland R. Rubber Compound and Tires Based on such a Compound. EP. Patent, 0501227A1, 1992.

[7] Bansal R C, Donnet J-B, Wang M-J. Chapter 2. Carbon Black, Science and Technology. New York: Marcel Dekker, Inc., 1993.

[8] Frianf G F, Thorley B. Carbon Black Process. U.S. Patent, 3010794, 1961.

[9] Rivin D, Smith R G. Environmental Health Aspects of Carbon Black. *Rubber. Chem. Technol.,* 1982, 55: 707.

[10] Krejci J C. Production of Carbon Black. U.S. Patent, 2564700, 1951.

[11] Heller G L. Vortex Reactor for Carbon Black Manufacture. U.S. Patent, 3490869, 1970.
[12] Belmont J A. Process for Preparing Carbon Materials with Diazonium Salts and Resultant Carbon Products. U.S. Patent, 5554739, 1996.
[13] Belmont J A, Amici R M, Galloway C P. Reaction of Carbon Black with Diazonium Salts, Resultant Carbon Black Products and Their Uses. U.S. Patent, 5851280, 1998.
[14] Belmont J A. Aqueous Inks and Coatings Containing Modified Carbon Products. U.S. Patent, 5672198, 1997.
[15] Belmont J A, Adams C E. Non-aqueous Inks and Coatings Containing Modified Carbon Products. U.S. Patent, 5713988, 1998.
[16] Belmont J A, Amici R M, Galloway C P. Reaction of Carbon Black with Diazonium Salts, Resultant Carbon Black Products and Their Uses. U.S. Patent, 6494946, 2002.
[17] Keoshkerian B, Georges M K, Drappel S V. Ink Jettable Toner Compositions and Processes for Making and Using. U.S. Patent, 5545504, 1996.
[18] Bansal R C, Donnet J-B. Chapter 4. Donnet J-B, Bansal R C, Wang M-J. Carbon Black, Science and Technology. New York: Marcel Dekker, Inc., 1993.
[19] Eisenmenger E, Engel R, Kuehner G, et al. Carbon Black Useful for Pigment for Black Lacquers. U.S. Patent, 4366138, 1982.
[20] Amon F H, Thornhill F S. Process of Making Hydrophilic Carbon Black. U.S. Patent, 2439442, 1948.
[21] Wolff S, Görl U. Carbon Blacks Modified with Organosilicon Compounds, Method of Their Production and Their Use in Rubber Mixtures. U.S. Patent, 5159009, 1992.
[22] Joyce G A, Little E L. Thermoplastic Composition Comprising Chemically Modified Carbon Black and Their Applications. U.S. Patent, 5708055, 1998.
[23] Mahmud K, Wang M-J, Francis R A. Elastomeric Compounds Incorporating Silicon-treated Carbon Blacks. U.S. Patent, 5830930, 1998.
[24] Mahmud K, Wang M-J, Francis R A. Elastomeric Compounds Incorporating Silicon-treated Carbon Blacks and Coupling Agents. U.S. Patent, 5877238, 1999.
[25] Mahmud K, Wang M-J. Method of Making a Multi-phase Aggregate Using a Multi-stage Process. U.S. Patent, 5904762, 1999.
[26] Mahmud K, Wang M-J. Method of Making a Multi-phase Aggregate Using a Multi-stage Process. U.S. Patent, 6211279, 2001.
[27] Mahmud K, Wang M-J, Kutsovsky Y. Method of Making a Multi-phase Aggregate Using a Multi-stage Process. U.S. Patent, 6364944, 2002.
[28] Wang M-J, Mahmud K, Murphy L J, et al. Carbon-silica Dual Phase Filler, a New Generation Reinforcing Agent for Rubber-Part I. Characterization. *Kautsch. Gummi Kunstst.,* 1998, 51: 348.
[29] Wang M-J, Kutsovsky Y, Zhang P, et al. New Generation Carbon-Silica Dual Phase Filler Part I. Characterization and Application to Passenger Tire. *Rubber Chem. Technol.,* 2002, 75: 247.
[30] Anand J N, Mills J E, Reznek S R. Silicone Rubber Compositions Incorporating Silicon-treated Carbon Blacks. U.S. Patent, 6020402, 2000.
[31] Reed T, Mahmud K. Use of Modified Carbon Black in Gas-phase Polymerizations. U.S. Patent, 5919855, 1999.
[32] Kawazura T, Kaido H, Ikai K, et al. Surface-treated Carbon Black and Rubber Composition Containing Same. U.S. Patent, 5679728, 1997.
[33] Mahmud K, Wang M-J, Reznek S R, et al. Elastomeric Compounds Incorporating Partially Coated Carbon Blacks. U.S. Patent, 5916934, 1999.

[34] Mahmud K, Wang M-J, Belmont J A, et al. Silica Coated Carbon Blacks. U.S. Patent, 6197274, 2001.
[35] Iler R K. The Chemistry of Silica. New York: Wiley, 1979.
[36] Chevallier Y, Morawski J C. Precipitated Silica Having Improved Morphological Characteristics and Process for the Production Thereof. U.S. Patent, 4590052, 1986.
[37] Thornhill F S. Method of Preparing Silica Pigments. U.S. Patent, 2940830, 1960.
[38] Ulrich G D. Aggregation and Growth of Submicron Oxide Particles in Flames. *J. Colloid Interf. Sci.,* 1982, 87: 257.
[39] Barthel H, Rösch L, Weis J. Organosilicon Chemistry II: From Molecules to Materials. Weinheim: VCH, 1996.
[40] Pratsinis S E. Flame Aerosol Synthesis of Ceramic Powders. *Prog. Energy Combust. Sci.,* 1998, 47: 197.
[41] Kratel G. Process for the Manufacture of Silicon Dioxide. U.S. Patent, 4108964, 1978.

2 Characterization of Fillers

Fillers are characterized by their chemical composition, micro-structure, morphology, and physical chemistry of the surface. Figure 2.1 and Figure 2.2 schematically show the basic structures of carbon black and synthetic silica, respectively. The primary dispersible unit of fillers is referred to as an "aggregate", that is, a discrete, rigid colloidal entity. It is the functional unit in well-dispersed systems. For most carbon blacks and synthetic silicas, the aggregate is composed of spheres that are fused together. These spheres are generally termed as primary "particles" or "nodules". While primary particles of silicas are composed of amorphous silicon dioxide, in carbon black aggregates, these nodules are composed of many tiny graphite-like stacks. Within the nodule of carbon blacks, the stacks are oriented so that their *c*-axis is normal to the sphere surface, at least near the nodule surface.

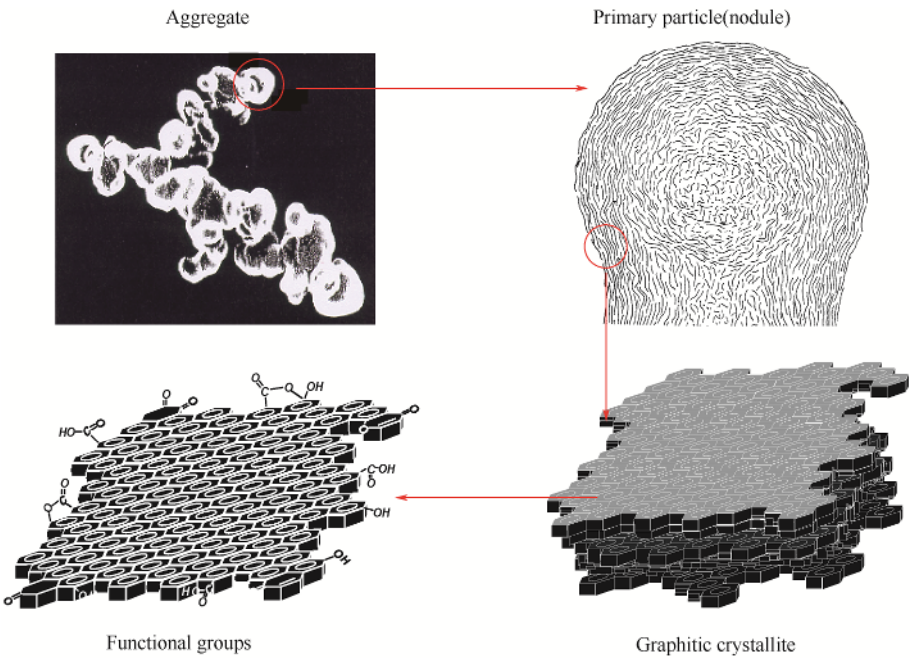

Figure 2.1 Structure of carbon black

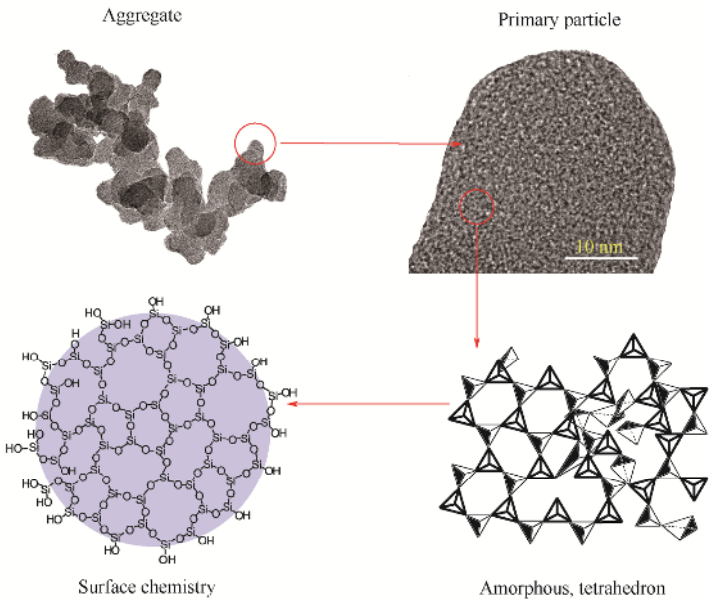

Figure 2.2 Structure of silica

■ 2.1 Chemical Composition

2.1.1 Carbon Black

Oil-furnace blacks used by the rubber industry contain over 97% elemental carbon. Thermal and acetylene blacks consist of over 99% carbon. Table 2.1 shows the chemical composition of some carbon blacks. Other elements included in furnace black, apart from carbon, are hydrogen, oxygen, sulfur, and nitrogen. In addition, there are mineral oxides, salts, and traces of adsorbed hydrocarbons. Hydrogen and sulfur are distributed on the surface and the interior of the aggregates. The oxygen content is located on the surface of the aggregates as C_xO_y complexes.

Table 2.1 Chemical composition of carbon blacks

Type	Carbon/ %	Hydrogen/ %	Oxygen/ %	Sulfur/ %	Nitrogen/ %	Ash/ %	Volatile/ %
Furnace rubber grade	97.3–99.3	0.20–0.80	0.20–1.50	0.20–1.20	0.05–0.30	0.10–1.00	0.60–1.50
Medium thermal	99.4	0.30–0.50	0.00–0.12	0.00–0.25	NA	0.20–0.38	–
Acetylene black	99.8	0.05–0.10	0.10–0.15	0.02–0.05	NA	0.00	<0.40

NA – not available.

Hydrocarbon materials produce carbon blacks; therefore, it is mostly hydrogen that saturates the dangling bonds at the edges of the basal planes of the graphitic layers. The graphitic layers are large, polycyclic aromatic ring systems.

Oxygen-containing complexes are by far the most important surface groups. The oxygen content of carbon blacks varies from 0.2% to 1.5% in mass for furnace blacks and 3% to 4% for channel blacks. Some special blacks used for pigment purposes contain larger quantities of oxygen than normal furnace blacks. These blacks are made by oxidation in a separate process step using nitric acid, ozone, air, or other oxidizing agents. They may contain from 2% to 12% oxygen. The oxygen-containing groups influence the physico-chemical properties, such as chemical reactivity, wettability, catalytic properties, electrical properties, and adsorbability. Oxidation improves dispersion and flow characteristics in pigment vehicle systems such as lithographic inks, paints, and enamels. In rubber-grade blacks, surface oxidation reduces pH and changes the kinetics of vulcanization, making the rubber compounds slower curing.

A convenient method for assessing the extent of surface oxidation is the measurement of volatile content. This standard method measures the weight loss of the evolved gases on heating up from 120°C to 950°C in an inert atmosphere. The composition of these gases consists of three principal components: hydrogen, carbon monoxide, and carbon dioxide. The volatile content of normal furnace blacks is under 1.5%, and the volatile content of oxidized special grades is 2% to 22%.

The origin of the volatile gases is the functional groups attached to carbon black, especially those on the surface. Surface oxides bound to the edges of the carbon layers are phenols, hydroquinones, quinones, neutral groups with one oxygen, carboxylic acids, lactones, and neutral groups containing two oxygens[1,2]. Figure 2.1 shows an idealized graphite-surface-layer plane with the various functional groups located at the periphery of the plane. Carbon blacks with few oxygen groups show basic surface properties and anion exchange behavior[3,4].

In addition to combined hydrogen and oxygen, carbon blacks may contain as much as 1.2% combined sulfur resulting from the sulfur content of the aromatic feedstock that contains thiophenes, mercaptans, and sulfides. The majority of the sulfur is not potentially reactive as it is inaccessibly bound in the interior of carbon black particles and does not contribute to sulfur cross-linking during the vulcanization of rubber compounds.

The nitrogen in carbon blacks is the residue of nitrogen heterocycles in the feedstocks. Thus, carbon blacks derived from coal tars have far more nitrogen than petroleum-derived blacks.

The ash content of furnace blacks is normally a few tenths of a percent but in some products may be as high as one percent. The chief source of ash is the water used to quench the hot black from the reactors during manufacture and for wet pelletizing the black.

2.1.2 Silica

Chemically, it is not the "ideal silica" with which we are concerned in reinforcing rubber. Wagner[5] in 1976 reviewed the chemistry and the micro-structure of silica. His review remains the best summary of silica chemistry.

Regarding silica composition, the purity of silicon dioxide is one parameter influencing rubber reinforcement, and such purities vary among production processes and post treatments. The purity of fumed silica is quite high, with a silica content of 98% or more, while precipitated silica is about 88%–92%. Impurities include silicate and Ca or Al elements among others; however, the main impurities are oxygen and hydrogen in the form of silanols with adsorbed and bonded water.

It has been found[6–10] that in an ideal state the surface silanol content is 4.6 OH groups per nm^2. This corresponds to the available surface silicon atoms permitted by the lattice configuration of silica. Lattice imperfections at the surface, and even within the bulky particle, permit values greater than 4.6 to occur. Incomplete silanol condensation and the presence of geminal hydroxyls (i.e., two hydroxyls on one silicon atom) are observed on freshly prepared, nonannealed silicas. Pyrogenic silicas approach the ideal state more closely than precipitated silicas. By the process of high-temperature dehydration and annealing (~450°C), followed by rehydration, both types approach this ideal state of 4.6 OH/nm^2.

Reports indicate[11] a considerable difference between the virgin surfaces of the two types of silicas. To begin with, precipitated silica strongly holds physically adsorbed water, causing high hydration. Whereas outgassing (in vacuum) at room temperature was sufficient at removing physically adsorbed water from fumed silica, a significant quantity of more strongly adsorbed water on precipitated silica was lost during heating from 25°C to 150°C. Readsorption of water indicates a hydroxyl concentration of 12.5 OH/nm^2, considerably higher than the ideal of 4.6. Similarly, readsorption of water on fumed silica (after vacuum outgassing) gives a value of 2.19 OH/nm^2, increased by rehydration to 3.31, still less than the "fully hydrated" condition proposed[8–10]. Furthermore, comparative isopropanol adsorption indicates that the hydroxyls on the precipitated silica surface are sufficiently close together that steric hindrance prevents a 1:1 interaction between silanol and isopropanol. The hydroxyls in fumed silica, even after rehydration, are sufficiently isolated to permit essentially equivalent site adsorption by water and isopropanol. Wang's findings show the hydroxyl concentration on precipitated silica reaching 19 OH/nm^2 when testing an alkylation of silica with methanol at 200°C[12]. This value decreases to 4 OH/nm^2 for fumed silica. Such high concentrations of OH groups on both silicas are attributed to the imperfection of silica lattice and micro-pore on the surface as the methanol treatments are performed under a very high pressure.

There is some evidence that adsorbed water may exist on silicas up to 300°C[13]. This may contribute to the very high hydroxyl concentration[11], since adsorbed water provides additional sites for further adsorption.

The silanol concentration at the surface depends on the number of silicon atoms per unit area at the surface and the number of hydroxyl groups presenting on each silicon atom. Amorphous silicas bear a close resemblance to silica glass, with a short-range order but with a random arrangement of more distant neighbors. For convenience, a resemblance to one or more faces of β-cristobalite or β-tridymite is postulated. The differences in surface silicon atoms between these two are small, 3.95 per nm^2 and 4.6 per nm^2, but the former can accommodate two hydroxyl groups to give 7.9 OH/nm^2. On the surface, silicon atoms in the other form can hold only one hydroxyl group, but the spatial arrangement could permit the second-layer silicons to participate, yielding either 4.6 OH/nm^2 or 13.8 OH/nm^2. As will be seen later, the evidence points to the value of 7.9 OH/nm^2 for fully hydrated amorphous silicas.

The number of surface hydroxyls does not fully characterize the silica surface. Their distribution and, particularly, the close proximity of hydroxyls have an influence on adsorption of polar molecules and, to some extent, their reactivity.

Three types of surface hydroxyls have been identified: isolated, vicinal (on adjacent silicon atoms), and geminal (two hydroxyls on the same silicon atom), which are schematically shown in Figure 2.3[6,14–16]. Even additional "anomalous adsorption sites" have been claimed[17].

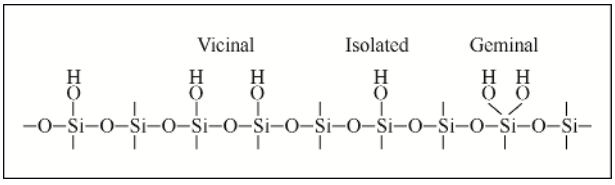

Figure 2.3 Type of silanols on silica surface

There is reason to believe that there are several types of adsorption sites attributed to hydroxyl configurations on the silica surface. Hockey and Pethica[18] present evidence from infrared spectroscopy and thermogravimetric analysis that geminal hydroxyls exist on fully hydrated, nonannealed surfaces. Incomplete silanol condensation between first- and second-layer surface silicon atoms forced the first-layer silicon to carry two hydroxyls. After annealing (above 400°C) geminal hydroxyls are no longer formed on rehydration.

Isolated hydroxyls, i.e., not interacting with near-neighbor hydroxyls, exist predominantly on extensively dehydrated surfaces. Fumed silicas and, to a much lesser extent, precipitated silicas have isolated hydroxyls. As the degree of hydration increases, the existence of isolated hydroxyls decreases, and vicinal hydroxyls increases[14].

This is significant for adsorption of water and other polar adsorbates. Adjacent silanols are more powerful adsorption sites for water than isolated silanols[13,14]. The same can be said for other polar chemicals. The heat of adsorption of methanol on silica

decreases significantly as the silica is heated from 105°C to 900°C[19], while that of the nonspecific adsorbate, carbon tetrachloride, does not. The favorable disposition of adjacent silanols apparently favors much stronger adsorption of polar species. This will be discussed in the characterization of filler surface with inverse gas chromatography.

2.2 Micro-Structure of Fillers

2.2.1 Carbon Black

The arrangement of carbon atoms in carbon black has been well-established by X-ray diffraction methods[20,21]. The diffraction patterns show diffuse rings at the same positions as diffraction rings from pure graphite. Heating carbon black to 3000°C further emphasizes the suggested relation to graphite. The diffuse reflections sharpen, but the pattern never approaches that of true graphite. Carbon black has a degenerated graphitic crystalline structure as defined above. Whereas graphite has a three-dimensional order, as seen in the model structures of Figure 2.4, carbon black has a two-dimensional order. The X-ray data indicate that carbon black consists of well-developed graphite platelets stacked roughly parallel to one another but random in orientation with respect to adjacent layers. As shown in Figure 2.4 the carbon atoms in the graphitic structure of carbon black form large sheets of condensed aromatic ring systems with an interatomic spacing of 0.142 nm within the sheet identical to that found in graphite. However, the interplanar distances are quite different. While graphite interplanar distance is 0.335 nm which results in a relative density of 2.26, the interplanar distance of carbon black is larger, in the range of 0.350–0.365 nm, as a consequence of the random planar orientations or so-called turbostratic arrangement. The relative density of commercial carbon blacks is 1.76–1.90 depending on the grade. About half of the decrease in density is attributed to stacking height, L_c, in the crystallites. X-ray diffraction data provide estimates of crystallite size. For a typical carbon black, the average crystallite diameter, L_a, is about 1.7 nm and average L_c is 1.5 nm, which corresponds to an average of four planal layers per crystallite containing ~375 carbon atoms.

It was originally suggested that these discrete crystallites were in random orientation within the particle. This view was later abandoned when electron microscopy of graphitized and oxidized carbon blacks indicated more of a concentric layer plane arrangement that can be described by a paracrystalline model. High resolution phase-contrast electron microscopy, which made possible the direct imaging of graphitic layers in carbon black, has confirmed this structure[22]. Figure 2.5 shows transmission electron micrographs of carbon black and graphitized blacks at high resolution. For carbon black, the image displays the marked concentric arrangement of the planal layers at the surface and around what appear to be growth centers. Upon heat treatment

of the carbon black in nitrogen atmosphere at high temperature, it seems that almost all of the carbon black atoms are graphitized.

The micro-structure of the carbon black surface has been investigated by means of scanning tunneling microscopy (STM)[23,24]. Figure 2.6 shows the STM images obtained in the current mode for graphite, graphitized carbon black and normal carbon black N234. Compared to graphite, the structure of carbon blacks graphitized for 24 hours at a temperature of 2700°C in an inert atmosphere still remains in a certain imperfect state, shown by different tunneling current patterns in the organized domains.

The surface structure of carbon black can be classified as two types: organized domains and unorganized domains. The organized domains occupy the majority of the carbon black surface, and their size generally decreases with decreasing particle size.

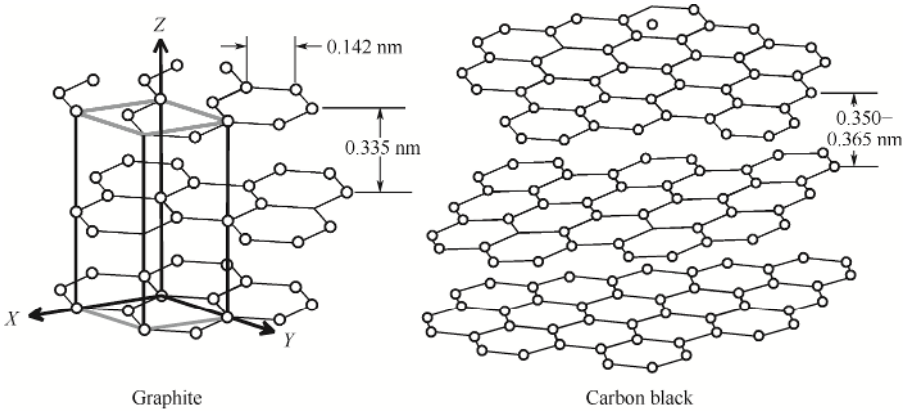

Figure 2.4 Atomic structural models of graphite and carbon black

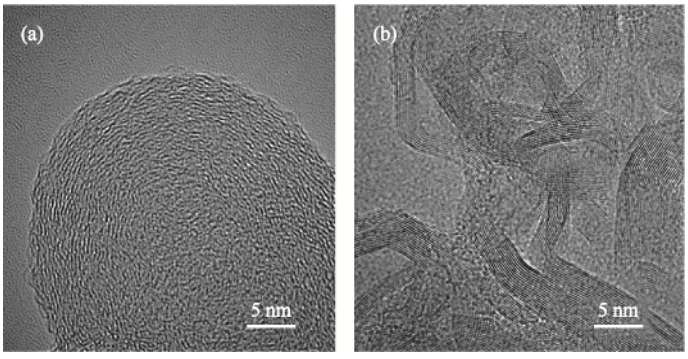

Figure 2.5 Comparison of the morphology and structure of carbon black samples: (a) before and (b) after heat treatment

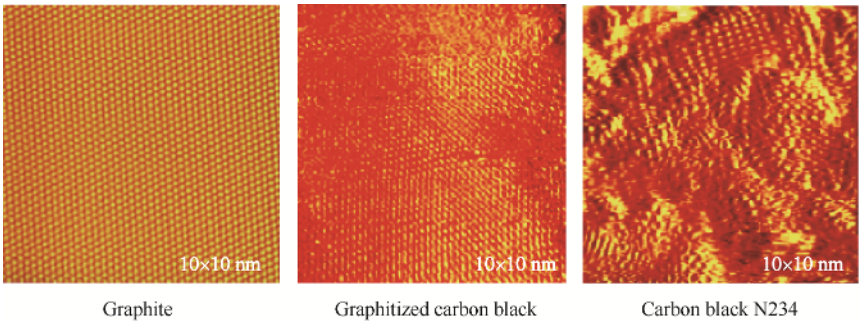

Figure 2.6 STM images of graphite, graphitized carbon black, and carbon black N234

2.2.2 Silica

Both precipitated and fumed silicas are amorphous materials that consist of silicon and oxygen tetrahedrally bound into an imperfect three-dimensional structure (Figure 2.2). The degree of lattice imperfection, which depends upon the conditions of synthesis, has several consequences. First, there is no long-range crystal order, only short-range, with a random arrangement of more distant neighbors. In this regard, it resembles silica glass. Secondly, imperfections within the lattice structure leave free silanol groups. These are evident in infrared and thermogravimetric studies, but are inaccessible to adsorption or reaction with external agents. Finally, the surface contains uncondensed silanols on a siloxane lattice, which has features of both the 100 face of β-cristobalite and 001 face of β-tridymite. The number of silanols, their distribution, and even the conformation of the surface siloxane lattice also depend on the synthetic method and thermal treatment.

The structure of amorphous silicas has been extensively studied with infrared spectroscopy, thermogravimetry, chemical reactivity, and specific adsorptivity. It has helped to semiquantitatively describe the silica surface structure, which is important to rubber reinforcement.

■ 2.3 Filler Morphologies

Besides their composition and micro-structure, fillers differ in their primary "particle" or nodule size, surface area, aggregate size, aggregate shape, and in the distribution of each of these. Morphology is a set of properties related to the average magnitude and frequency distribution of their sizes and the way primary particles are connected in the aggregates.

2.3.1 Primary Particles – Surface Area

Although the smallest discrete entity of filler is the aggregate, the "particle" size, and its distribution is one of the most important morphological parameters with regard to its

end-use applications, even though the particles do not exist as discrete entities except for thermal black and some special non-black fillers. The particle size is directly related to the specific surface area as the latter increases exponentially with the decrease of the former. It is an extensive parameter in rubber compounds and determines the interfacial area between rubber and filler, because rubber compounding is always based on the weight of materials. It is therefore of critical importance to the specific surface area of the fillers and has been taken as the principal parameter for grade classification of rubber fillers. In almost all types of carbon blacks and silicas, the primary particles within a single aggregate are similar. However, the types of fillers can differ in the uniformity of the primary particles of different aggregates. While many types show a quite narrow range of primary particles, others are clearly quite broad mixtures of aggregates of different primary particle size or specific surface area. The electron microscope is the universally accepted instrument for measuring particle size, surface area, aggregate size, and aggregate morphology, but the adsorption methods, both gas- and liquid-phase adsorptions, are convenient and accurate measurements for specific surface area.

2.3.1.1 Transmission Electron Microscope (TEM)

Almost all filler aggregates used in the rubber industry, particularly the tire industry, are nano-scale sized and the classification of the various grades of carbon blacks is based on the size of the primary particles, which determines the surface area of the filler. TEM examination alone has made it possible to measure the particle size and aggregate morphology, as it can reach a nanometric resolution and, in combination with image analytical procedures, allows a two-dimensional statistical analysis.

Figure 2.7 and Figure 2.8 show typical electron micrographs of rubber-grade carbon blacks and precipitated silicas.

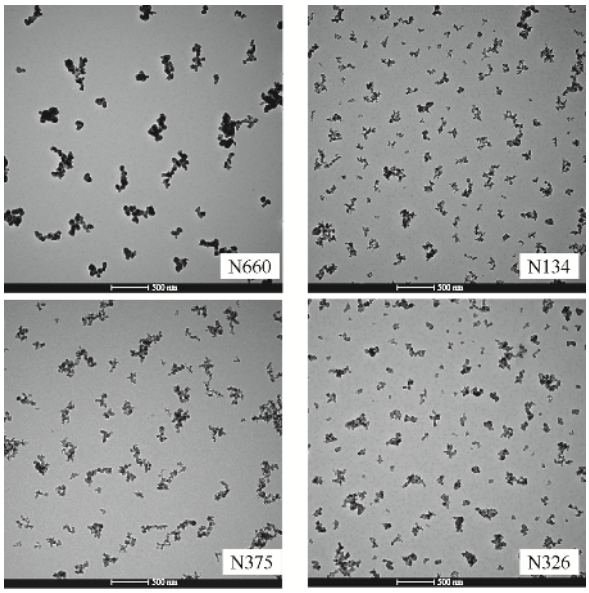

Figure 2.7 Electron micrographs of rubber-grade carbon blacks

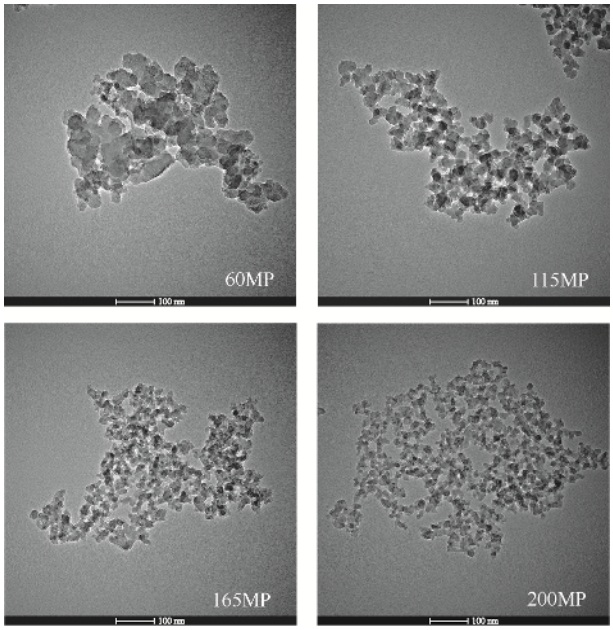

Figure 2.8 Electron micrographs of rubber-grade precipitated silicas

The major limitations to the morphological analysis of fillers are related to the low speed of operation and to the complexity of aggregates under investigation. Therefore, many attempts have been made to speed up the data processing from the morphological images.

Nowadays, the potential of TEM has been greatly enhanced by the possibility of using automated image analysis (AIA), which allows acquisition of structural details and quantitative information on the filler through the use of descriptors based on geometrical parameters, such as size, volume of the primary particles and aggregates, and morphological parameters, describing the shape of the aggregates such as asymmetry and bulkiness.

Hess, Ban, and McDonald, in 1969, fully automated the analysis of carbon black particle and aggregate size in a dry state[24]. A Quantimet (QTM) performed the analyses, which were based on a television scanning device able to directly analyze a microscopic image. Later, in 1974, they reported a more practical automated size analysis method for carbon black[25], which is part of the ASTM procedure D3849.

Since then, many new imaging and analyzing systems have been developed commercially, and the techniques of image analysis have rapidly evolved due to progress in image acquisition and development of algorithms and software, either for general or specific applications. For these reasons more reliable and quantitative results on the morphology of fillers can be obtained which was reviewed by Conzatti, Costa, Falqui, and Turturro[26]. TEM micrographs provide digitalized images; the automated image analyzers provide measurements of the area and perimeter of an

individual aggregate. Based on the two parameters, a variety of parameters characterizing the size and morphology of the aggregate and particle can be derived.

Shown in Figure 2.9 is the image of a carbon black aggregate, its area, A, that is, the projected area, and perimeter, P.

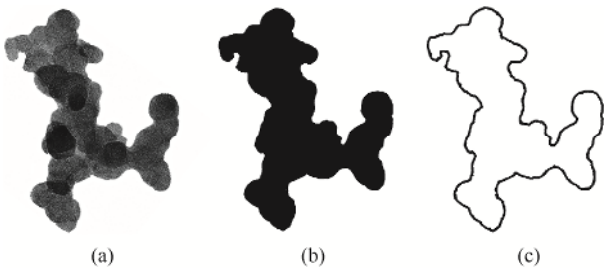

Figure 2.9 Image of (a) a carbon black aggregate, (b) its area, and (c) its perimeter

According to Hess and McDonald[27], an average particle size, d_p (nm) determines each individual aggregate using the mean chord length, $\pi A/P$:

$$d_p = \alpha \pi A/P \tag{2.1}$$

where α is an aggregation factor to correct for the fact that the mean chord is usually a measure of the average distance across multiple particles. To achieve more accurate average particle size measurements within each pigment aggregate, an equation for self-determination of α was developed. This is expressed as:

$$\lg \alpha = C_1 \lg\left(P^2/A\right) + C_2 \tag{2.2}$$

where P^2/A is a nondimensional aggregate irregularity factor, and C_1 and C_2 are constants based on the slope and intercept of the relationship. Means of correlations such as that shown in Figure 2.10 empirically established the general form of the equation. This plots P^2/A against calculated values for α. Eq. 2.3 is fine-tuned for C_1 and C_2 using a series of non-porous carbon blacks with well-established size and surface area data. C_1 and C_2 are varied systematically to give the best overall data fit, but with the restriction that all equations must give the correct value of α for a perfect sphere ($4/\pi$). The value for a sphere is greater than one because the diameter actually represents the longest chord. The P^2/A value for the projection of a sphere is equal to 4π. The values established for the C_1 and C_2 constants are −0.92 and 1.117, respectively. With these constants, Eq. 2.2 can be converted to:

$$\alpha = 13.092\left(P^2/A\right)^{-0.92} \tag{2.3}$$

With this equation, no size cutoffs are required using Eq. 2.1 to calculate d. However, it was found to be desirable to limit the lower value of α to 0.45. It can be seen that the P^2/A curve (Figure 2.10) flattens out in this general region. The 0.45 lower limit was determined in the same manner as C_1 and C_2. With no limitations on α, the higher

moments of the particle size distribution are relatively unaffected, but the number average values tend to be on the low side. The use of the 0.45 limit also permits application of the equation to the screening of dry blacks and blacks extracted from rubber compounds. When the calculated α is lower than 0.4, use $\alpha = 0.4$.

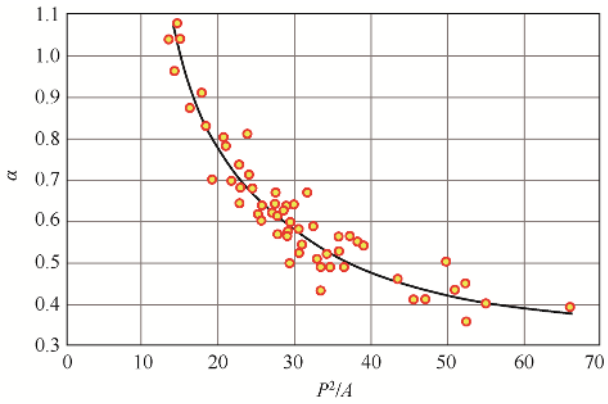

Figure 2.10 Calculated α *vs.* P^2/A[27]

For one filler, the particle size mean diameter, d_{sm} (nm), can be calculated based on the d_p of several thousand aggregate images of known magnification as:

$$d_{sm} = \Sigma(nd_p^3)/(nd_p^2) \tag{2.4}$$

The electron microscope surface area, EMSA (m^2/g), can be obtained by:

$$\text{EMSA} = 6000/(\rho d_{sm}) \tag{2.5}$$

where ρ is the filler density, which is assumed to be 1.8 g/cm^3 for carbon black.

Generally, for rubber-grade carbon blacks, the surface areas determined by TEM are in reasonable agreement with surface areas determined by nitrogen adsorption measurements. However, for those carbon blacks that have highly developed micro-pores, particularly special pigment blacks and blacks used for electrical conductivity, the surface areas calculated from their particle diameters are smaller than those calculated from gas absorption, as the internal surface area in the micro-pore is excluded.

Therefore, compared with BET surface area (NSA), the EMSA value is closer to STSA, the external surface area measured with nitrogen adsorption, because in the TEM measurement, the microscope is set at a magnification to obtain surface values that are similar to STSA (see Section 2.3.1.2.2).

It should be pointed out that the TEM method is the only way to obtain the particle size distribution which may be related to certain what in rubber properties of fillers.

2.3.1.2 Gas Phase Adsorptions

While TEM images contain very detailed statistical information, using this method to obtain the surface area of the filler is expensive and time consuming. Direct measurement of specific surface area is much faster and less expensive. Gas- and liquid-phase adsorption, which depend on the amount of adsorbate required to form a surface monolayer, are simple techniques to make such measurements. If the area occupied by a single-adsorbate molecule is known, a simple calculation will yield the surface area.

For gas adsorption, the amount of gas adsorbate on solid adsorbent is a function of the mass of the solid, temperature, gas pressure, and nature of both gas and solid. The adsorption isotherms are classified into five types according to the theory of Brunauer, Emmett, and Teller[28], as shown in Figure 2.11. The isotherm type Ⅰ, also known as Langmuir isotherm, has a monolayer adsorption, i.e., further adsorption cannot take place on the adsorbed molecules. However, for most adsorbate-adsorbent systems, especially for the fillers used in elastomers, at temperatures not far from their condensation points, the adsorption isotherms of gases show two regions for most adsorbents: at low pressures, the isotherms are concave, at higher pressures convex toward the pressure axis (type Ⅱ). Such isotherms are believed to indicate the formation of multimolecular adsorbed layers. The BET equation, based on Brunauer et al.'s multimolecular adsorption, is the only theory able to explain all types of adsorption.

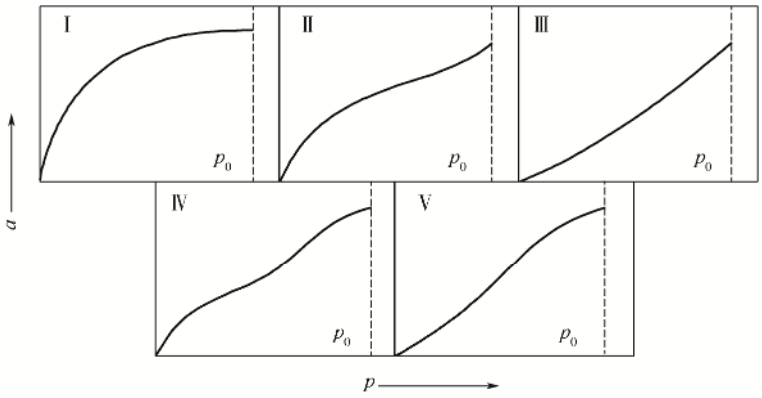

Figure 2.11 Multilayer adsorption of gas molecules[28]

ASTM has adopted as standard method D6556, a low-temperature nitrogen-adsorption process, based on the original method of Brunauer, Emmett, and Teller (BET)[29]. This method is not susceptible to changes in the surface chemistry of carbon black such as those resulting from surface oxidation and the presence of trace amounts of tarry materials. With a molecular diameter of less than 0.5 nm, nitrogen is small enough to enter the micro-pore space so that the surface measured by BET is the total area, including micro-pores. For some applications, such as rubber reinforcement, the internal

surface area in micro-pores with less than 2 nm diameter is inaccessible to large rubber molecules, thus it has no effect or has a negative effect on rubber reinforcement. The specific surface area that is accessible to rubber is defined as "external" surface area. This is conveniently measured by a multilayer nitrogen adsorption, also defined in ASTM D6556 and known as the statistical thickness surface area (STSA)[30].

2.3.1.2.1 Total Surface Area Measured by Nitrogen Adsorption – BET/NSA

The BET theory assumes that not only does the adsorbate-adsorbent interaction determine the adsorption of gases on the adsorbent, but also the interaction between adsorbate molecules. This implies that when the adsorbate molecules in a gas state collide with those adsorbed on the adsorbent they may also be adsorbed on the solid surface, resulting in multimolecular adsorption. This is schematically shown in Figure 2.12.

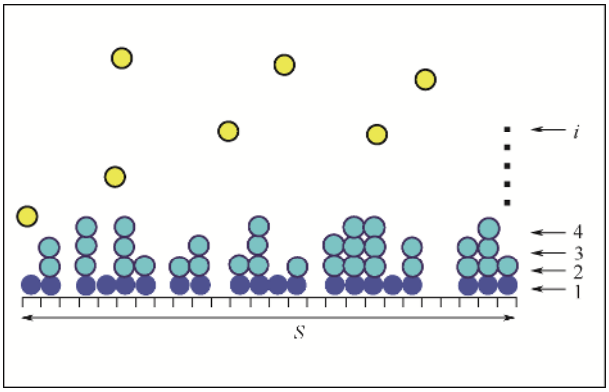

Figure 2.12 Multilayer adsorption of gas molecules

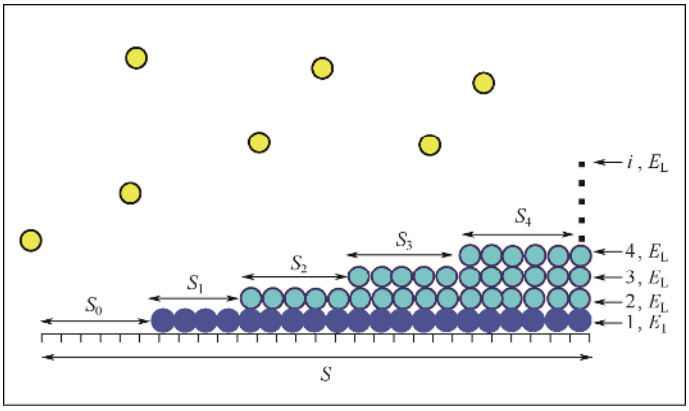

Figure 2.13 Schematic multilayer adsorption and interaction energy of different layers

As shown in Figure 2.13, at a given pressure, S_0, S_1, S_2, ..., S_i represent the surface area covered by 0, 1, 2, ..., i layers of adsorbate. When the adsorption is at equilibrium, S_0 must remain constant. In this case, the adsorption rate of gas molecules on the bare surface is

equal to the rate of desorption of the adsorbed adsorbate from the first layer. While the adsorption rate of the gas is proportional to the pressure, p, and the bare surface area, S_0, the desorption rate of the adsorbed adsorbate is in proportion with the number of molecules that are able to evaporate from the monolayer. According to Boltzmann's law, if the heat of adsorption of the first layer is E_1, this number is directly proportional to $\exp(-E_1/RT)$, in which R is the gas constant and T is the temperature. Thus, one has:

$$a_1 p S_0 = b_1 S_1 \mathrm{e}^{-E_1/RT} \tag{2.6}$$

where a_1 and b_1 are constants that are assumed to be independent of the number of molecules adsorbed already in the first layer.

S_1 can change in four different ways: by adsorption on the bare surface, by desorption from the first layer, by condensation on the first layer, and by evaporation from the second layer. At equilibrium adsorption, S_1 must also remain constant. Thus obtained is:

$$a_2 p S_1 + b_1 S_1 \mathrm{e}^{-E_1/RT} = b_2 S_2 \mathrm{e}^{-E_2/RT} + a_1 p S_0 \tag{2.7}$$

where the constants a_2, b_2, and E_2 are similarly defined to a_1, b_1, and E_1. From Eqs. 2.6 and 2.7, it follows that:

$$a_2 p S_1 = b_2 S_2 \mathrm{e}^{-E_2/RT} \tag{2.8}$$

This suggests that the adsorption rate on the top of the first layer is also equal to that of desorption rate from the second layer. Applying the same argument to the second and consecutive layers, it follows:

$$a_3 p S_2 = b_3 S_3 \mathrm{e}^{-E_3/RT} \ldots \tag{2.9}$$

and

$$a_i p S_{i-1} = b_i S_i \mathrm{e}^{-E_i/RT} \tag{2.10}$$

The total surface area of the solid, S, and the total volume adsorbed, V, are given by:

$$S = S_0 + S_1 + S_2 + \cdots + S_i = \sum_{i=0}^{\infty} S_i \tag{2.11}$$

and

$$V = V_0 \left(S_1 + 2S_2 + \cdots + iS_i \right) = V_0 \sum_{i=1}^{\infty} iS_i \tag{2.12}$$

where V_0 is the volume of gas adsorbed on a unit surface area of the adsorbent when it is covered with a complete mono-molecular layer of adsorbate. Therefore,

$$\frac{V}{SV_0} = \frac{V}{V_{\mathrm{m}}} = \frac{\sum_{i=1}^{\infty} iS_i}{\sum_{i=0}^{\infty} S_i} \tag{2.13}$$

where V_m is the volume of gas adsorbed when the entire adsorbent surface is adsorbed with a complete mono-molecular layer.

The summations indicated in Eq. 2.13 are performed if two simplifying assumptions are made as:

$$E_2 = E_3 = \cdots = E_i = E_L \tag{2.14}$$

E_L being the heat of liquefaction of the adsorbate, and

$$\frac{b_2}{a_2} = \frac{b_3}{a_3} = \cdots = \frac{b_i}{a_i} = K \tag{2.15}$$

where K is an appropriate constant.

This suggests that the adsorption-desorption properties of the molecules in the second and higher adsorbed layers are the same as evaporation-condensation properties, which are the same as those of the liquid state of adsorbate. This is reasonable since the only adsorbed molecules that directly contact the solid surface are those in the first layer. From the second layer, all adsorbed molecules are in contact with the same type of molecules and they are not or are much less influenced by the solid surface. Supposing

$$x = \frac{p}{K} e^{E_L/RT} \tag{2.16}$$

and

$$y = \frac{a_1}{b_1} p e^{E_1/RT} \tag{2.17}$$

it was obtained:

$$S_1 = yS_0 \tag{2.18}$$

$$S_2 = xS_1 \tag{2.19}$$

$$S_3 = xS_2 = x^2 S_1 \tag{2.20}$$

and

$$S_i = xS_{i-1} = x^{i-1} S_1 = yx^{i-1} S_0 \tag{2.21}$$

Therefore, one has:

$$S_i = Cx^i S_0 \tag{2.22}$$

where

$$C \equiv \frac{y}{x} = \frac{a_1 K}{b_1} e^{(E_1 - E_L)/RT} \tag{2.23}$$

Substituting Eq. 2.22 into Eq. 2.13, one has:

$$\frac{V}{V_m} = \frac{CS_0 \sum_{i=1}^{\infty} i x^i}{S_0 \left(1 + C \sum_{i=1}^{\infty} x^i\right)} \tag{2.24}$$

The summation represented in the denominator is merely the sum of an infinite geometric progression:

$$\sum_{i=1}^{\infty} x^i = \frac{x}{1-x} \tag{2.25}$$

Concerning the summation in the numerator, it can be expressed by:

$$\sum_{i=1}^{\infty} i x^i = x \frac{\mathrm{d}}{\mathrm{d}x} \sum_{i=1}^{\infty} x^i = \frac{x}{(1-x)^2} \tag{2.26}$$

It is the case, therefore, that

$$\frac{V}{V_m} = \frac{Cx}{(1-x)(1-x+Cx)} \tag{2.27}$$

When the adsorption takes place on a free surface, at the saturation pressure of the gas, p_0, an infinite number of layers can build up on the adsorbent, i.e., $V \to \infty$. According to Eq. 2.27, to make $V = \infty$ at $p = p_0$, x must be equal to unity, i.e.,

$$\frac{p_0}{K} \mathrm{e}^{E_1/RT} = 1 \tag{2.28}$$

and

$$x = \frac{p}{p_0} \tag{2.29}$$

where x is relative pressure. Substituting it into Eq. 2.27, the adsorption isotherm can be expressed as:

$$V = \frac{V_m C p}{(p_0 - p)\left[1 + (C-1)\frac{p}{p_0}\right]} \tag{2.30}$$

which is the famous two-constant BET equation.

If the thickness of the adsorption layers cannot exceed some finite number, n, such as on a porous surface, then the summation of the two series in Eq. 2.24 is limited to n terms only, and not to infinity. In this case, Eq. 2.27 becomes:

$$\frac{V}{V_m} = \frac{Cx}{(1-x)}\left[\frac{1-(n+1)x^n + nx^{n+1}}{1+(C-1)x - Cx^{n+1}}\right] \tag{2.31}$$

This is the three-constant BET equation. For $n = 1$, i.e., monolayer adsorption, Eq. 2.31 can be simplified to:

$$V = V_m \frac{C}{p_0} p / \left(1 + \frac{C}{p_0} p\right) \tag{2.32}$$

which is the Langmuir equation of monolayer adsorption.

Eq. 2.31 represents the first three types of adsorption isotherms reported by Brunauer et al.[28]. If $n = 1$, it is a type 1 isotherm. When $E_1 > E_L$, it is type 2. Isotherm type 3 represents the case of $E_1 < E_L$. Types 4 and 5 indicate, besides multilayer adsorption, the involvement of capillary condensation, which, as discussed later, does not influence the BET equation to the surface area measurement of powders.

Application of BET Equation to Surface Area Measurements

Although there are some arguments about the difference between the assumptions of BET theory and actual situations, it does not seem to show any significant effect on its application in surface area measurement. Such arguments are mainly related to the adsorption energies, such as the energetic heterogeneity and the interaction between the second layer with the adsorbent surface, even though the contribution of the latter to the adsorption energy of the second layer is very small, since it reduces exponentially with distance. Generally, distribution of the surface energies of the adsorbent is quite heterogeneous, and the adsorption energy of the second layer should be influenced by the surface energies of the solid. This is especially true for adsorption at very low pressure. At relatively higher coverage of the adsorbent, at least for the surface coverage between 0.5−1.5 that is calculated by V/V_m, the intermolecular interaction of the adsorbed molecules can significantly compensate the effects of the surface heterogeneity. When Eq. 2.30 is used, this may be the reason why the applicable range of relative pressure, p/p_0, is 0.05−0.35 for surface measurement, which corresponds to the surface coverage of 0.5−1.5.

If V_m at standard temperature and pressure (STP) and the effective cross-sectional area of the adsorbate, σ_a, at the adsorption temperature are obtained, the surface area of solid (NSA) in m^2/g can be calculated according to the equation:

$$\text{NSA} = 4.35 V_m \tag{2.33}$$

where 4.35 is the area occupied by 1 cm^3 of nitrogen in STP.

Measurement of V_m

For the purpose of testing, Eq. 2.30 can be written in the linearity form:

$$\frac{p}{V(p_0 - p)} = \frac{1}{V_m C} + \frac{C-1}{V_m C} \times \frac{p}{p_0} \tag{2.34}$$

Plotting $p/V(p_0 - p)$ against p/p_0 should give a straight line whose slope, M, is $(C - 1)/V_m C$ and intercept, B, is $1/V_m C$. From M and B, the V_m and C can be calculated from:

$$V_m = \frac{1}{M + B} \tag{2.35}$$

and

$$C = \frac{M}{B} + 1 \tag{2.36}$$

It has been demonstrated that between relative pressures, p/p_0, of 0.05 and 0.35, the experimental data fits Eq. 2.34 quite well.

The test can be done with different adsorbates, such as argon[31], krypton[32], xenon[33], propane[34], and butane[35]. For the fillers used in rubbers, the unique and reliable measurement has been performed with adsorption of nitrogen at its boiling point (−196°C).

Generally, multiple points are taken from the range of relative pressure from 0.05 to 0.35 for calculation. In fact, for nitrogen adsorption, a set of data having p/p_0 in the range of 0.05 to 0.3 are used to calculate the V_m and C value. However, for most adsorbates, the intercepts of the straight-line plots of Eq. 2.34, $1/V_mC$, are small.

For simplification, a so-called "single point" method may be used. In this case, the slopes of the straight line connecting one pressure point to the origin of the straight-line plots can determine V_m. This standard test method measures the surface area based on a single partial pressure of 0.30 kPa ± 0.01 kPa. The time required to run a single point test is less than that of the multi-point test, but can be less accurate due to the effect of the surface properties. However, because the equipment and test are simpler, it may be adequate for quality control depending on the requirements of the producer and the customer.

Using a classical glass vacuum apparatus to measure the adsorption isotherms of nitrogen adsorption is a time-consuming and expensive operation. Another method for building up isotherms is based on selective adsorption of nitrogen from a mixture with other gases, helium in particular. This technique does not require a vacuum system and is time saving as the adsorption equilibrium is established rapidly[36]. Nelsen and Eggertsen[37–39] further developed this method using a so-called continuous flow chromatography. In this technique, a nitrogen/helium mixture passes through the filler in a sample cell that is immersed in liquid nitrogen. When the adsorption is complete, the liquid nitrogen reservoir is quickly removed and the sample cell is placed in a heating mantle. A thermal conductivity detector disrobes and records the change in the adsorbed nitrogen. From the resulting peak area, the volume of nitrogen adsorption is calculated. Varying the concentration of the mixture determines the adsorption isotherm point by point.

Calculation of σ_a

After the value of V_m is obtained, the average area by each molecule on the surface, σ_a, is required to calculate the surface area of the adsorbent. σ_a may not be the actual molecular size of the adsorbate. Even for the same type of adsorbate, this value may somewhat vary due to changes in adsorption states, such as the adsorption temperature and the surface properties of adsorbents.

Generally, the adsorbed layers can be treated as a liquid. Therefore, the molecular area, σ_a, from liquid density is established based on the spherical model in the most dense face-centered packing[40], e.g.,

$$\sigma_a = 1.091 \times 10^{16} \left(\frac{M_W}{\rho N_A} \right)^{2/3} \tag{2.37}$$

where M_W is the molecular weight of the adsorbate, ρ the density of the adsorbate at experimental temperature, and N_A Avogadro's number.

According to Eq. 2.37 the molecular area of nitrogen, σ_a, used for surface area calculation is 16.2 Å^2 (1 Å = 10^{-10} m) as the density of nitrogen at the adsorption temperature (−196°C) is 0.808 g/cm^3. This value is in agreement with those obtained by the same adsorbents with known surface areas.

It should be pointed out that before the surface area can be determined, it is necessary to remove any material that may already be on the surface. Removal of this material (usually by heating under a vacuum) is essential; otherwise two potential errors are possible. The first error can affect the mass, and the second error can interfere with the nitrogen's access to the adsorbent surface.

2.3.1.2.2 External Surface Area Measured by Nitrogen Adsorption − STSA

Specific surface area is an important property for filler grade classification, production control, and prediction of rubber reinforcement characteristics. It is generally accepted that some internal area arises from micro-pores that are available to nitrogen which is commonly used in evaluating surface area, but they do not appear to be accessible to elastomer molecules. Therefore, this part of the area does not contribute to application performance. The NSA or total surface area alone is insufficient for estimating the reinforcing properties of microporous fillers. Thus, in predicting performance from area measurements, one should consider the external area.

Nitrogen adsorption isotherms at −196°C have been used extensively to calculate pore sizes and size distribution in carbon blacks[41−46]. These analyses are based on comparisons of the isotherms of the samples under investigation with those from standard planes of non-porous surfaces.

Originally, the comparison was made by plotting the nitrogen isotherms on a reduced basis, i.e., V_a/V_m, where V_a is the equilibrium volume and V_m the monolayer volume (all in cm^3 at normal temperature and pressure), as a function of relative nitrogen pressure p/p_0. If the reduced isotherm of the standard non-porous adsorbent superposes on that of the sample, one may then conclude that the sample is also non-porous. Departure from the standard isotherm was interpreted in terms of micro-pore filling[44,45].

Later, a so-called *t* procedure was proposed in which the volume, V_a, of N_2 adsorbed by the sample at relative pressure p/p_0 can be transformed to functions of *t*, the statistical thickness of the adsorbed nitrogen layer at the same p/p_0 read from the reduced isotherm of the standard. The term, *t*, is called the statistical layer thickness due to the fact that the